

CERN-EP-2024-148
27 May 2024

Measurement of ${}^3_{\Lambda}\text{H}$ production in Pb–Pb collisions at $\sqrt{s_{\text{NN}}} = 5.02$ TeV

ALICE Collaboration*

Abstract

The first measurement of ${}^3_{\Lambda}\text{H}$ and ${}^3_{\Lambda}\bar{\text{H}}$ differential production with respect to transverse momentum and centrality in Pb–Pb collisions at $\sqrt{s_{\text{NN}}} = 5.02$ TeV is presented. The ${}^3_{\Lambda}\text{H}$ has been reconstructed via its two-charged-body decay channel, i.e., ${}^3_{\Lambda}\text{H} \rightarrow {}^3\text{He} + \pi^-$. A Blast-Wave model fit of the p_{T} -differential spectra of all nuclear species measured by the ALICE collaboration suggests that the ${}^3_{\Lambda}\text{H}$ kinetic freeze-out surface is consistent with that of other nuclei. The ratio between the integrated yields of ${}^3_{\Lambda}\text{H}$ and ${}^3\text{He}$ is compared to predictions from the statistical hadronisation model and the coalescence model, with the latter being favoured by the presented measurements.

arXiv:2405.19839v1 [nucl-ex] 30 May 2024

© 2024 CERN for the benefit of the ALICE Collaboration.

Reproduction of this article or parts of it is allowed as specified in the CC-BY-4.0 license.

*See Appendix A for the list of collaboration members

1 Introduction

Relativistic heavy-ion collisions provide a rich environment for the study of nuclei, hypernuclei, and their charge conjugates. Hypernuclei are nuclei that have at least one hyperon among their constituents. The additional strange baryon leads to a unique nuclear system that can help to benchmark the interactions among hyperons and nucleons. Understanding such interactions has become particularly relevant in recent years due to their important connections with the modeling of the equation-of-state of dense astrophysical objects, such as the neutron stars [1, 2]. In fact, a precise knowledge of the two-body (Y–N) and three-body (Y–N–N) hyperon–nucleon forces allows for determining whether the presence of hyperons in the innermost core of neutron stars, which is known to be energetically favourable, reconciles with the recent observations of large-mass neutron stars [3, 4]. Multiple studies analysing particle momentum correlations [5, 6] play a direct role in establishing these interactions. In a complementary approach, the lifetime and the binding energy of a hypernucleus reflect the strength of the Y–N and Y–N–N forces [7–9].

The lightest known hypernucleus is the hypertriton (${}^3_{\Lambda}\text{H}$), composed of a proton, a neutron, and a Λ hyperon. As such, it represents the simplest system to study the interaction among Λ hyperons and nucleons. Early experiments studied ${}^3_{\Lambda}\text{H}$ using nuclear emulsions and helium bubble chambers [10–14]. These experiments obtained results with large statistical uncertainties. In recent years, more precise measurements have been performed by ALICE [15–18] and STAR [19–21] Collaborations in relativistic heavy-ion collisions at the CERN LHC and BNL RHIC colliders. Such measurements contributed in determining that the ${}^3_{\Lambda}\text{H}$ is a loosely bound state with a Λ separation energy, B_{Λ} , of the order of one hundred keV, and has an average lifetime very close to the free Λ one [22]. With such properties, the hypertriton wave function is expected to have a radial extension of approximately 5 fm [23–25], considerably larger than the other nuclei with a mass number equal to three and comparable in size to the fireball created in Pb–Pb collisions.

There are two main classes of models used to explain the formation of nuclei in Pb–Pb collisions: the statistical hadronisation model (SHM) and the coalescence model. While the SHM is insensitive to the structure of the particle being produced [26–29], the coalescence model relies on the knowledge of the particle wave function to produce predictions [30–36]. There is a wealth of variations for each class of models but based on similar approach. In the SHM, the production cross section of a specific particle is determined solely by a temperature, denoted as chemical freeze-out temperature, the volume of the system created in the collision, the quantum numbers, and the mass of the particle. In Pb–Pb collisions, the grand canonical formulation of the SHM has proven to be very successful in describing the yields of light flavoured hadrons [26]. Based on the two parameters from the analysis of light hadrons, the SHM then provides a parameter-free prediction of the yields of (hyper)nuclei. In the coalescence model, the production rate of nuclei is given by the convolution between the phase space of the nucleons produced in the collision and the nuclear wave function, according to the Wigner function formalism [37]. These two models give similar predictions for the yield ratios of most ordinary nuclei (e.g. d/p) [32–34] and qualitatively describe the available experimental data at the LHC [38–49]. However, when it comes to a tight configuration or a loosely-bound state, the prediction of the SHM and the coalescence model for particle ratios diverge significantly in all collision systems. For example, recent studies on the yield of ${}^4\text{He}$ in Pb–Pb collisions show an agreement with the SHM while the coalescence model failed to explain it [49]. Conversely, the ${}^3_{\Lambda}\text{H}/\Lambda$ ratio in p–Pb collisions [17] is only well-described by the coalescence predictions. This discrepancy indicates that the nucleosynthesis mechanism [50, 51] still needs further investigation with new experimental measurements.

This letter presents the first measurement of the ${}^3_{\Lambda}\text{H}$ production in Pb–Pb collisions at a center-of-mass energy per nucleon pair $\sqrt{s_{\text{NN}}} = 5.02$ TeV. In Sec. 2 the ALICE apparatus and the analysis method are described, whereas the results are discussed in Sec. 3.

2 The ALICE detector and analysis details

The ALICE apparatus is composed of several specialised detectors, as detailed in [52]. In this analysis, ${}^3_{\Lambda}\text{H}$ are reconstructed using both the Inner Tracking System (ITS) [53] and the Time Projection Chamber (TPC) [54] detectors. The ITS is the closest central-barrel detector to the beam pipe and comprises six cylindrical layers. The primary role of ITS is to reconstruct charged-particle trajectories and to measure precisely the position of the interaction vertices. The TPC is a gaseous detector employed as the primary tracking and particle identification (PID) device in ALICE. The TPC is used to identify charged particles by measuring their specific energy loss. Both ITS and TPC are placed in a homogeneous magnetic field of 0.5 T produced by a solenoidal magnet. These two detectors cover the entire azimuth in the pseudorapidity range $|\eta| < 0.9$. The centrality determination and trigger are provided by a pair of forward ($2.8 < \eta < 5.1$) and backward ($-3.7 < \eta < -1.7$) detectors called V0A and V0C [55], respectively. The coincidence of a signal in the V0A and a signal in the V0C is used as a minimum-bias trigger. Additionally, two thresholds on the minimum amount of charge deposited on the V0 detector are implemented to trigger online on central and semi-central Pb–Pb collisions. These thresholds are defined by the Glauber model fit to the V0 detector signal amplitudes [55, 56].

The data sample employed in this analysis has been collected during the LHC 2018 Pb–Pb run at $\sqrt{s_{\text{NN}}} = 5.02$ TeV. Based on the signal amplitudes of the V0 detectors, three centrality classes are considered (from central to peripheral collisions): 0–10%, 10–30%, and 30–50%. The centrality classes are labeled according to the corresponding percentiles of the Pb–Pb hadronic interaction cross section. The stored events, categorized into the 0–10% and 30–50% classes, are enriched by the online trigger on central and semi-central collisions. In total, approximately 210 million events are studied. At the LHC energies, approximately the same number of ${}^3_{\Lambda}\text{H}$ and ${}^3_{\bar{\Lambda}}\text{H}$ are produced [57]. Therefore, the results of ${}^3_{\Lambda}\text{H}$ and ${}^3_{\bar{\Lambda}}\text{H}$ are averaged. In the following, we use the notation ${}^3_{\Lambda}\text{H}$ for both particle and antiparticle.

A dedicated Monte Carlo (MC) simulated sample has been employed for optimising the ${}^3_{\Lambda}\text{H}$ selection and evaluating the efficiency corrections. The MC sample consists of ${}^3_{\Lambda}\text{H}$ signal injected on top of underlying Pb–Pb collisions, which are simulated with the HIJING event generator [58]. In each MC event, 80 ${}^3_{\Lambda}\text{H}$ are injected. The transverse momentum (p_{T}) distribution of the injected signal is given by the Blast-Wave [59] function, with parameters taken from fit to the ${}^3\text{He}$ p_{T} spectra [48]. The particle transport through the detector material is done using GEANT4 [60], which simulates both the interaction with the material and the weak decay kinematics of the ${}^3_{\Lambda}\text{H}$.

In this analysis, ${}^3_{\Lambda}\text{H}$ candidates are reconstructed via the two-charged-body mesonic decay channel ${}^3_{\Lambda}\text{H} \rightarrow {}^3\text{He} + \pi^-$ (and the related charge conjugated process). Firstly, a preselection method is performed. Tracks that have specific energy loss in the TPC compatible within 5σ to that of ${}^3\text{He}$ or π tracks are employed to reconstruct the ${}^3_{\Lambda}\text{H}$ decay topology with the algorithm used in previous analyses [15–17]. The reconstruction of ${}^3_{\Lambda}\text{H}$ candidates employed the ALICE secondary vertex finder method which pairs opposite-sign ${}^3\text{He}$ and π candidate tracks. The tracks are required to have more than 50 hits in TPC ($N_{\text{cls}}^{\text{TPC}}$) and good fit quality ($\chi^2/N_{\text{cls}}^{\text{TPC}} < 4$). In order to mitigate the contamination from ${}^3\text{He}$ produced in the interaction with materials, an additional selection $p_{\text{T}} > 1.2$ GeV/ c is imposed for ${}^3\text{He}$. Additional selection criteria are used by combining data on the decay kinematics and the position of the decay vertex. The selections include the maximum distance-of-closest-approach (DCA) of the decay products to the primary vertex ($\text{DCA}_{\text{toPV}} < 8$ cm) and among the daughter tracks themselves ($\text{DCA}_{\text{tracks}} < 1.6$ cm), and the cosine of the angle between the ${}^3_{\Lambda}\text{H}$ momentum vector and the straight line connecting the primary and secondary vertices ($\cos\theta_{\text{p}}$). The selection on $\cos\theta_{\text{p}}$ is set as a function of the proper decay time of the candidates such to ensure a 95% efficiency for reconstructing true ${}^3_{\Lambda}\text{H}$.

The main selection step consists of combining the candidate features in a gradient-boosted decision tree classifier (BDT) [61, 62] that is employed for the ${}^3_{\Lambda}\text{H}$ signal selection. The BDT is a supervised learning algorithm that determines how to differentiate between two or more classes, specifically signal

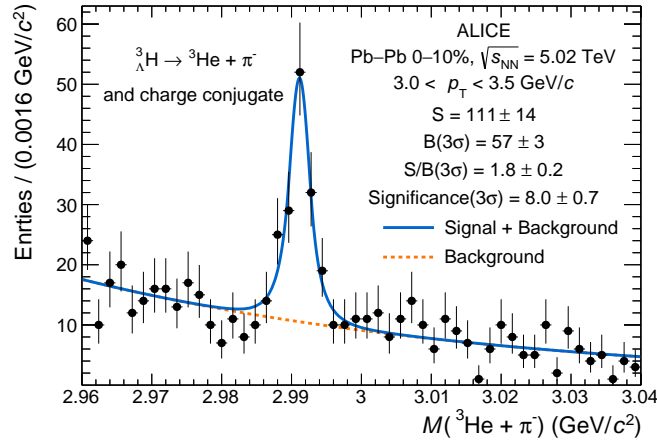


Figure 1: Invariant-mass distribution of selected ${}^3_{\Lambda}\text{H}$ candidates in the centrality class 0–10% and p_{T} interval $3 < p_{\text{T}} < 3.5$ GeV/ c fitted with a function which is the sum of a double-sided Crystal Ball signal and an exponential background. Vertical lines represent the statistical uncertainties.

and background in this context, by analysing sets of examples referred to as the training sets. In this analysis, the training sets consist of ${}^3_{\Lambda}\text{H}$ signal candidates obtained from the MC sample and background candidates from paired like-sign ${}^3\text{He}$ and π tracks from the data. For each ${}^3_{\Lambda}\text{H}$ candidate, the BDT combines a set of topological and single-track variables to produce a score, which serves to separate signal and background. The variables do not exhibit correlation with the ${}^3\text{He}-\pi$ invariant mass and are: the decay length in the rest frame ct , the $\cos\theta_{\text{p}}$, the PID information for ${}^3\text{He}$, the DCA to the primary vertex for both ${}^3\text{He}$ and π tracks, the DCA between ${}^3\text{He}$ and π , and the number of clusters of the ${}^3\text{He}$ track in the TPC. Candidates with a BDT score exceeding a specified threshold are classified as signal. This threshold is determined to optimise the expected signal significance, taking into account the predicted production yield according to the SHM for the ${}^3_{\Lambda}\text{H}$, as well as the background rate observed from like-sign ${}^3\text{He}$ and π pairs.

The BDT training and testing steps and the ${}^3_{\Lambda}\text{H}$ yield computation have been performed in different centrality and p_{T} intervals independently. The ${}^3_{\Lambda}\text{H}$ signal is extracted from the invariant-mass distribution after rejecting candidates whose score is lower than the BDT model threshold. An unbinned maximum-likelihood fit is performed to the ${}^3_{\Lambda}\text{H}$ invariant-mass distribution, employing a double-sided Crystal Ball (DSCB) [63] function and an exponential function to model the signal and the background components of the spectrum, respectively. The parameters of the DSCB function are fixed using the MC sample leaving only the mean and the normalisation of the DSCB free. Figure 1 shows an example of the invariant-mass fit in the most central collisions and in the p_{T} interval $3 < p_{\text{T}} < 3.5$ GeV/ c . The number of detected ${}^3_{\Lambda}\text{H}$ is obtained from the integral of the DSCB function. However, this number has to be corrected to account for the detection efficiency, the branching ratio (B.R.), and the absorption of the ${}^3_{\Lambda}\text{H}$ in the ALICE detector material. The detection efficiency comprises several components, including the acceptance of the ALICE detector, the absorption of daughter tracks, and the selection efficiency. It can be directly computed using the MC sample in different centrality and p_{T} intervals. The detection efficiency increases with the ${}^3_{\Lambda}\text{H}$ p_{T} and ranges from 10% to 38%. The branching ratio is set to 0.25 ± 0.023 according to Ref. [7]. Finally, the absorption correction (C_{abs}) is computed by simulating the interaction of ${}^3_{\Lambda}\text{H}$ with the ALICE detector material with GEANT4, and evaluating the probability (P_{abs}) of the ${}^3_{\Lambda}\text{H}$ to be absorbed before decaying. The absorption cross section employed for the simulation has been extracted from Ref. [64], which accounts for the extension of the ${}^3_{\Lambda}\text{H}$ wave function, and amounts to about 1.5 times that of the ${}^3\text{He}$. The probability of ${}^3_{\Lambda}\text{H}$ to be absorbed is found to be increasing as a function of p_{T} due to the larger amount of material crossed by the high-momentum particle. The

corresponding correction, computed as $C_{\text{abs}} = 1 - P_{\text{abs}}$, ranges from 0.96 to 0.93.

The main systematic uncertainties on the measurement of the ${}^3_{\Lambda}\text{H}$ p_{T} spectra are due to the ${}^3_{\Lambda}\text{H}$ decay reconstruction, the BDT selection, and the invariant-mass fit in each p_{T} interval. These systematic uncertainties are estimated as an envelope by employing a multi-trial approach. In this approach, the following elements of the analysis are varied: two different weak-decay vertex-reconstruction methods, two different background datasets for the BDT training, two different fit functions for the ${}^3_{\Lambda}\text{H}$ signal (a Kernel Density Estimator [65] and the DSCB), three different fit functions for the combinatorial background modelling (polynomial of the first and second order, and an exponential function), and different BDT selection thresholds (giving rise to a $\pm 10\%$ variation of the efficiency around its nominal value). These elements are varied incoherently to populate a distribution of different yields that constitute our trial distribution in each p_{T} and centrality interval. The systematic uncertainty is then estimated as the standard deviation of the obtained distributions and varies from 8% to 34% in different intervals. Since the absorption cross section of ${}^3_{\Lambda}\text{H}$ is uncertain, an additional uncertainty due to the absorption is evaluated by changing the interaction cross section in the simulation to three times the ${}^3\text{He}$ inelastic cross section with the detector materials. This results in systematic uncertainties of 4%–6%, depending on the p_{T} interval. Another source of the uncertainty originates from the uncertainty on the branching ratio, which amounts to 9% and is common to all the p_{T} and centrality classes.

3 Results and Discussions

The ${}^3_{\Lambda}\text{H}$ p_{T} -differential spectra in different centrality intervals, defined as the average of particles and antiparticles, are shown in Fig. 2 along with the spectra of deuterons, antitritons, and ${}^3\text{He}$ in the corresponding centrality ranges, as measured in Ref. [48]. A simultaneous fit with the Blast-Wave model parameterisation [59] is done with all the shown spectra. The parameters of the combined Blast-Wave fit are listed in Table 1. Notably, the temperature and velocity in the Blast-Wave fit are compatible with those obtained by fitting only light nuclei (d, t, ${}^3\text{He}$, ${}^4\text{He}$) [49], suggesting a similar kinetic freeze-out surface for light-flavoured nuclei.

Individual Blast-Wave fits are employed to extrapolate the ${}^3_{\Lambda}\text{H}$ spectrum in the unmeasured p_{T} range and obtain the total yield (dN/dy) in the three centrality classes. The variation intervals of the fit parameters are restricted to an interval of $\pm 1\sigma$ around the parameters obtained from the combined fits shown in Fig. 2. The resulting dN/dy values are reported in Table 1. The fraction of extrapolated yield using the Blast-Wave fit is 13%, 39%, and 27% for the 0–10%, 10–30%, and 30–50% centrality classes, respectively. The total uncertainties on the integrated yields $\sigma(\text{BW}_{\text{tot}})$ are computed by fitting the spectra considering both statistical and systematic uncertainties. To separate the statistical and systematic components of the uncertainty which originates from the Blast-Wave extrapolation, a fit considering only statistical uncertainty of the ${}^3_{\Lambda}\text{H}$ spectra is used to estimate the statistical component ($\sigma(\text{BW}_{\text{stat}})$). The systematic uncertainty due to the fitting procedure is extracted using the relation $\sigma(\text{BW}_{\text{syst}}) = \sqrt{\sigma(\text{BW}_{\text{tot}})^2 - \sigma(\text{BW}_{\text{stat}})^2}$. An additional source of systematic uncertainty to the measured yield arises from the unknown p_{T} distribution of ${}^3_{\Lambda}\text{H}$. As the fits performed with other functions, namely m_{T} -exponential and Boltzmann, have not passed the Pearson χ^2 test for the goodness of the fit and since the p_{T} distribution of ${}^3_{\Lambda}\text{H}$ should be very similar to ${}^3\text{He}$ according to the Blast-Wave model [59], the related uncertainty is inherited from the previous ${}^3\text{He}$ production analysis [48] and corresponds to 1.8%, 3.3%, and 0.3% of the measured integrated yield in 0–10%, 10–30%, 30–50%, respectively.

The production yield of ${}^3_{\Lambda}\text{H}$ provides a powerful tool to investigate the mechanism of nuclear production in relativistic hadronic collisions [18]. The measured ${}^3_{\Lambda}\text{H}$ yield in all the centrality intervals is directly compared with the predictions from the grand-canonical SHM [66] with $T=155$ MeV. The predicted ${}^3_{\Lambda}\text{H}$ dN/dy (9.5×10^{-5}) is approximately two times higher than the measured one in central Pb–Pb collisions, suggesting that the SHM, as applied, may lack certain elements necessary for accurately describing the

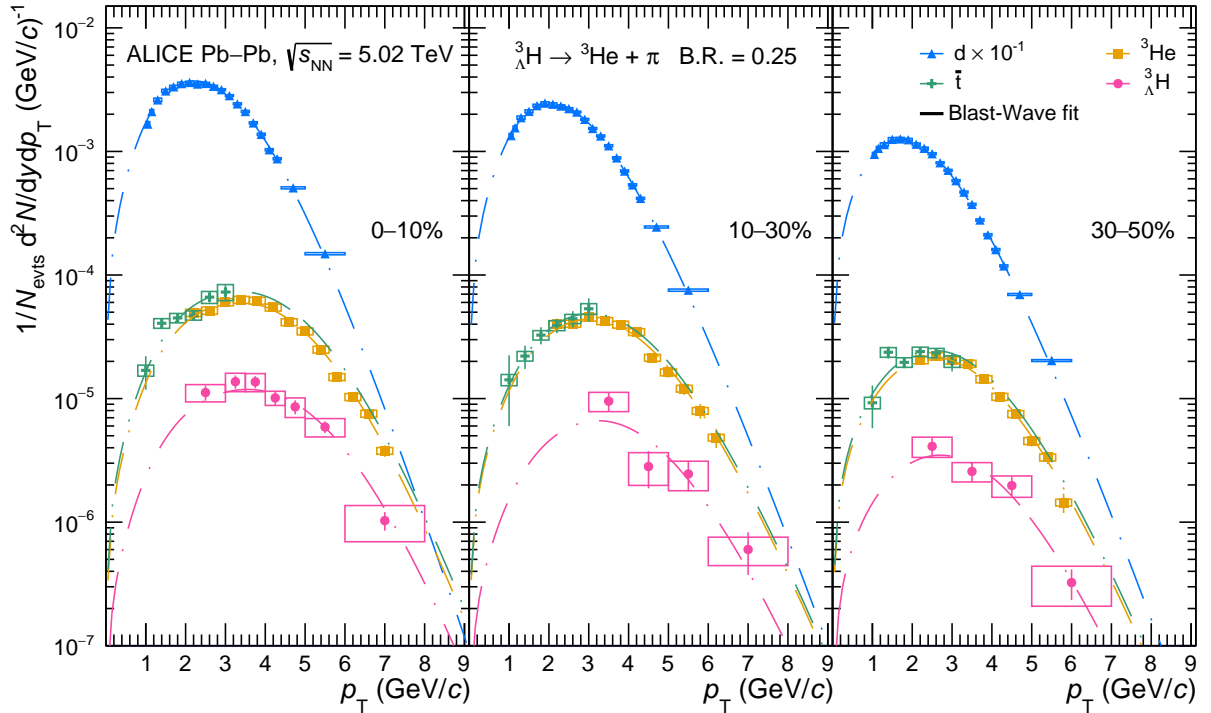


Figure 2: Deuteron (d), antitriton (\bar{t}), ${}^3\text{He}$ [48], and ${}^3_{\Lambda}\text{H}$ spectra measured in Pb–Pb collisions at $\sqrt{s_{\text{NN}}} = 5.02$ TeV. Each panel shows a centrality interval and different nuclei are reported with different colours. For ${}^3_{\Lambda}\text{H}$, the average spectra between particles and antiparticles is employed. The boxes represent the systematic uncertainties, while the vertical lines are the statistical ones. The combined Blast-Wave fit parameters for d , \bar{t} , ${}^3\text{He}$, and ${}^3_{\Lambda}\text{H}$ are listed in Table 1.

Table 1: Parameters of the combined Blast-Wave fits and integrated $({}^3_{\Lambda}\text{H} + {}^3_{\Lambda}\bar{\text{H}})/2$ yields in different centrality intervals. The fits include deuteron, antitriton, ${}^3\text{He}$, and ${}^3_{\Lambda}\text{H}$ as shown in Fig. 2. The ${}^3_{\Lambda}\text{H}$ yields are obtained with an individual Blast-Wave fit whose parameters are restricted in 1σ region of the parameters shown in the table.

Centrality	$\langle\beta_{\text{T}}\rangle$	T (GeV)	n	χ^2 / ndf	$dN/dy \times 10^{-5}$ (B.R. = 0.25)
0–10%	0.694 ± 0.003	0.103 ± 0.005	0.498 ± 0.009	43.4 / 39	$4.83 \pm 0.23(\text{stat}) \pm 0.57(\text{syst})$
10–30%	0.666 ± 0.003	0.132 ± 0.008	0.507 ± 0.012	19.1 / 34	$2.62 \pm 0.25(\text{stat}) \pm 0.40(\text{syst})$
30–50%	0.598 ± 0.005	0.152 ± 0.010	0.660 ± 0.022	21.8 / 33	$1.27 \pm 0.10(\text{stat}) \pm 0.14(\text{syst})$

generation of this weakly bound state.

On the other hand, while the SHM is able to calculate directly the absolute yields of hadrons, in the coalescence model only the yield ratios among particles can be computed without any further knowledge of the momentum spectra of the nucleons. To compare with both the models, SHM and coalescence, the ${}^3_{\Lambda}\text{H}/{}^3\text{He}$ ratio is considered. The produced charged-particle multiplicities per unit of pseudorapidity $\langle dN_{\text{ch}}/d\eta \rangle$, which are related to the centrality of the collision and can reflect the size of the fireball, may have effects on the ratios of particle yields and need to be taken into account. In this case, the grand-canonical SHM predicts no multiplicity dependence. A deviation from the grand-canonical ensemble prediction is present in the canonical SHM only for $\langle dN_{\text{ch}}/d\eta \rangle_{|\eta| < 0.5} < 100$ [27], which corresponds to peripheral collisions comparatively and is not covered by the presented results. The coalescence model formulation here considered [67] uses the Wigner function formalism and a parametrisation of the wave function of the ${}^3_{\Lambda}\text{H}$ that depends on its Λ separation energy. Three different coalescence predictions are shown by setting B_{Λ} to the latest ALICE and STAR experimental values and to the world average of the B_{Λ} measurements [18, 20, 22]. The uncertainty due to the B_{Λ} value is asymmetric as the ${}^3_{\Lambda}\text{H}$

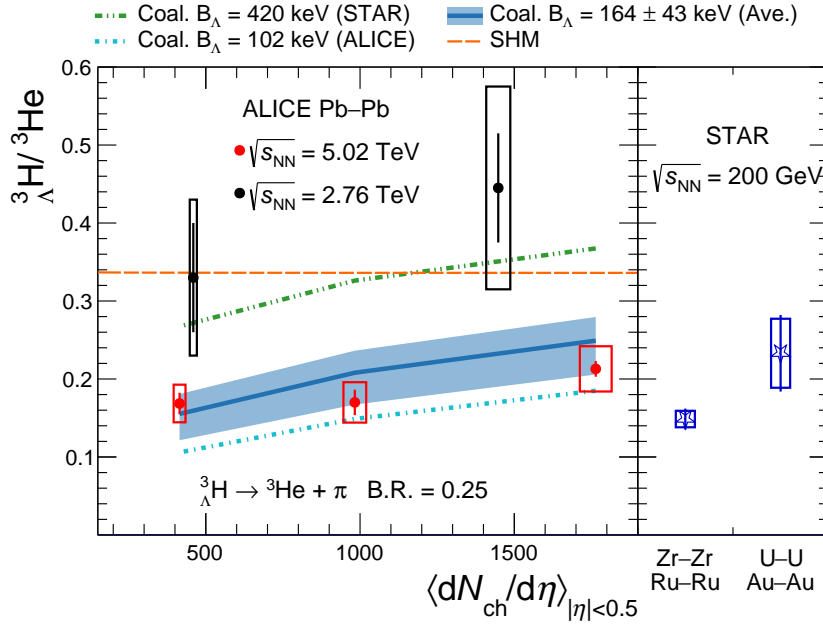


Figure 3: Yield ratio of ${}^3_{\Lambda}\text{H}$ to ${}^3\text{He}$ together with theoretical predictions as a function of multiplicity. In the left panel, the results of this analysis are compared with the ALICE measurement at $\sqrt{s_{\text{NN}}} = 2.76$ TeV [15]. Vertical lines are used for the statistical uncertainties and boxes for the systematic ones. For each centrality interval the $\langle dN_{\text{ch}}/d\eta \rangle$ is taken from Ref. [68] and the ${}^3\text{He}$ yield from Ref. [48]. The dense orange dashed line represents the expectation of SHM, while the other three sets of lines stand for coalescence model with different B_{Λ} hypotheses. The coalescence prediction with world average B_{Λ} is displayed with a 1σ uncertainty as the filled area, both lines and shadowed areas are linear interpolations of the available model calculations [67]. In the right panel, the results of recent STAR measurement are shown for comparison [21].

wave function width is not a linear function of B_{Λ} . Furthermore, the coalescence model predicts a suppression of the ${}^3_{\Lambda}\text{H}/{}^3\text{He}$ ratio with decreasing multiplicities due to the interplay between the smaller hadron emission source in peripheral Pb–Pb collisions and the wide wave function of the ${}^3_{\Lambda}\text{H}$. In Fig. 3, the model predictions are compared with the measured ${}^3_{\Lambda}\text{H}/{}^3\text{He}$ yield ratio as a function of the average charged-particle multiplicity of the analysed centrality intervals. The measured ${}^3_{\Lambda}\text{H}/{}^3\text{He}$ yield ratios are well described by the coalescence prediction using the current world average of B_{Λ} (solid blue line). In addition, the recent STAR measurements [21] suggest a similar suppression of the ${}^3_{\Lambda}\text{H}/{}^3\text{He}$ ratio going from large (Au–Au and U–U) to smaller (Zr–Zr and Ru–Ru) collision systems. For larger values of B_{Λ} , the predictions from the coalescence model approach that of the SHM, but they are not compatible with the measured ratios. The results from a prior ALICE analysis [15] in Pb–Pb collisions at $\sqrt{s_{\text{NN}}} = 2.76$ TeV are included in Fig. 3 for comparison. The results presented in this Letter remain consistent with the previous study within a 2σ confidence interval, but uncertainties are twice as small as those obtained from the smaller data sample at lower collision energy.

In Fig. 4, the ${}^3_{\Lambda}\text{H}/{}^3\text{He}$ yield ratio as a function of p_{T} in the three different centrality intervals is shown. While the SHM does not infer the expected p_{T} shape of the particles, the coalescence mechanism implies a decrease of the ${}^3_{\Lambda}\text{H}/{}^3\text{He}$ ratio for increasing p_{T} . Conversely, in a simple hydrodynamic picture like the Blast-Wave model, the radial flow boosts the high p_{T} production of heavier particles such as the ${}^3_{\Lambda}\text{H}$. Consequently, within the Blast-Wave framework, the ${}^3_{\Lambda}\text{H}/{}^3\text{He}$ ratio is expected to increase as a function of p_{T} . However, the current experimental uncertainties do not allow for a definitive conclusion on the trend of the ${}^3_{\Lambda}\text{H}/{}^3\text{He}$ ratio as a function of p_{T} .

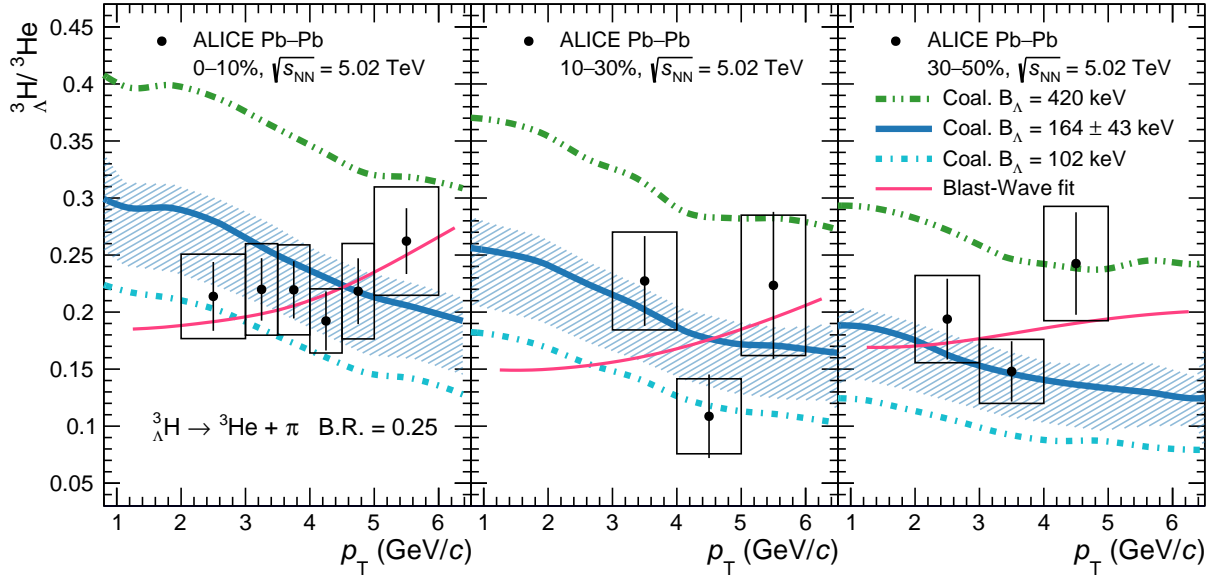


Figure 4: The ${}^3_{\Lambda}\text{H}/{}^3\text{He}$ yield ratio together with theoretical predictions in different centrality intervals as a function of p_{T} . The vertical lines and boxes represent the statistical and systematic uncertainties, respectively. The pink solid lines are calculated as the ratios of the Blast-Wave fit functions for ${}^3\text{He}$ and ${}^3_{\Lambda}\text{H}$. The other three curves stand for the predictions of the coalescence model with different B_{Λ} hypotheses. The coalescence prediction with world average B_{Λ} is displayed with a 1σ uncertainty band [67].

4 Conclusions

This Letter presents the first p_{T} -differential measurement of the ${}^3_{\Lambda}\text{H}$ production in Pb–Pb collisions at $\sqrt{s_{\text{NN}}} = 5.02$ TeV. The p_{T} distribution of ${}^3_{\Lambda}\text{H}$ is well described by a simultaneous Blast-Wave fit with other light nuclei. The fit temperature and velocity profiles are compatible with those found for other light-flavoured nuclei, hinting to a common kinetic freeze-out surface for hypernuclei and ordinary nuclei produced in Pb–Pb collisions. The p_{T} -integrated yields show a significant discrepancy with respect to the predictions of the SHM tuned to fit the other light-flavoured particles. Furthermore, the yield ratio ${}^3_{\Lambda}\text{H}/{}^3\text{He}$ was calculated to test the predictions of the coalescence model, that is able to describe the measured ratios when assuming the correct binding energy of the ${}^3_{\Lambda}\text{H}$. Finally, both the coalescence and the Blast-Wave models describe the experimental data for the ${}^3_{\Lambda}\text{H}/{}^3\text{He}$ ratios as a function of p_{T} . However, their predictions have a different p_{T} trend. Presently, the large experimental uncertainties preclude a definitive interpretation; however, the forthcoming data from LHC Run 3 will allow the ALICE Collaboration to measure this quantity with unprecedented precision.

Acknowledgements

The ALICE Collaboration would like to thank all its engineers and technicians for their invaluable contributions to the construction of the experiment and the CERN accelerator teams for the outstanding performance of the LHC complex. The ALICE Collaboration gratefully acknowledges the resources and support provided by all Grid centres and the Worldwide LHC Computing Grid (WLCG) collaboration. The ALICE Collaboration acknowledges the following funding agencies for their support in building and running the ALICE detector: A. I. Alikhanyan National Science Laboratory (Yerevan Physics Institute) Foundation (ANSL), State Committee of Science and World Federation of Scientists (WFS), Armenia; Austrian Academy of Sciences, Austrian Science Fund (FWF): [M 2467-N36] and Nationalstiftung für Forschung, Technologie und Entwicklung, Austria; Ministry of Communications and High Technologies, National Nuclear Research Center, Azerbaijan; Conselho Nacional de Desenvolvimento Científico e Tecnológico (CNPq), Financiadora de Estudos e Projetos (Finep), Fundação de Amparo à

Pesquisa do Estado de São Paulo (FAPESP) and Universidade Federal do Rio Grande do Sul (UFRGS), Brazil; Bulgarian Ministry of Education and Science, within the National Roadmap for Research Infrastructures 2020-2027 (object CERN), Bulgaria; Ministry of Education of China (MOEC), Ministry of Science & Technology of China (MSTC) and National Natural Science Foundation of China (NSFC), China; Ministry of Science and Education and Croatian Science Foundation, Croatia; Centro de Aplicaciones Tecnológicas y Desarrollo Nuclear (CEADEN), Cubaenergía, Cuba; Ministry of Education, Youth and Sports of the Czech Republic, Czech Republic; The Danish Council for Independent Research | Natural Sciences, the VILLUM FONDEN and Danish National Research Foundation (DNRF), Denmark; Helsinki Institute of Physics (HIP), Finland; Commissariat à l’Energie Atomique (CEA) and Institut National de Physique Nucléaire et de Physique des Particules (IN2P3) and Centre National de la Recherche Scientifique (CNRS), France; Bundesministerium für Bildung und Forschung (BMBF) and GSI Helmholtzzentrum für Schwerionenforschung GmbH, Germany; General Secretariat for Research and Technology, Ministry of Education, Research and Religions, Greece; National Research, Development and Innovation Office, Hungary; Department of Atomic Energy Government of India (DAE), Department of Science and Technology, Government of India (DST), University Grants Commission, Government of India (UGC) and Council of Scientific and Industrial Research (CSIR), India; National Research and Innovation Agency - BRIN, Indonesia; Istituto Nazionale di Fisica Nucleare (INFN), Italy; Japanese Ministry of Education, Culture, Sports, Science and Technology (MEXT) and Japan Society for the Promotion of Science (JSPS) KAKENHI, Japan; Consejo Nacional de Ciencia (CONACYT) y Tecnología, through Fondo de Cooperación Internacional en Ciencia y Tecnología (FONCICYT) and Dirección General de Asuntos del Personal Académico (DGAPA), Mexico; Nederlandse Organisatie voor Wetenschappelijk Onderzoek (NWO), Netherlands; The Research Council of Norway, Norway; Pontificia Universidad Católica del Perú, Peru; Ministry of Science and Higher Education, National Science Centre and WUT ID-UB, Poland; Korea Institute of Science and Technology Information and National Research Foundation of Korea (NRF), Republic of Korea; Ministry of Education and Scientific Research, Institute of Atomic Physics, Ministry of Research and Innovation and Institute of Atomic Physics and Universitatea Nationala de Stiinta si Tehnologie Politehnica Bucuresti, Romania; Ministry of Education, Science, Research and Sport of the Slovak Republic, Slovakia; National Research Foundation of South Africa, South Africa; Swedish Research Council (VR) and Knut & Alice Wallenberg Foundation (KAW), Sweden; European Organization for Nuclear Research, Switzerland; Suranaree University of Technology (SUT), National Science and Technology Development Agency (NSTDA) and National Science, Research and Innovation Fund (NSRF via PMU-B B05F650021), Thailand; Turkish Energy, Nuclear and Mineral Research Agency (TENMAK), Turkey; National Academy of Sciences of Ukraine, Ukraine; Science and Technology Facilities Council (STFC), United Kingdom; National Science Foundation of the United States of America (NSF) and United States Department of Energy, Office of Nuclear Physics (DOE NP), United States of America. In addition, individual groups or members have received support from: Czech Science Foundation (grant no. 23-07499S), Czech Republic; European Research Council (grant no. 950692), European Union; ICSC - Centro Nazionale di Ricerca in High Performance Computing, Big Data and Quantum Computing, European Union - NextGenerationEU; Academy of Finland (Center of Excellence in Quark Matter) (grant nos. 346327, 346328), Finland.

References

- [1] J. Schaffner-Bielich, “Hypernuclear Physics for Neutron Stars”, *Nucl. Phys. A* **804** (2008) 309–321, [arXiv:0801.3791 \[astro-ph\]](#).
- [2] L. Tolos and L. Fabbietti, “Strangeness in Nuclei and Neutron Stars”, *Prog. Part. Nucl. Phys.* **112** (2020) 103770, [arXiv:2002.09223 \[nucl-ex\]](#).
- [3] D. Lonardonì, A. Lovato, S. Gandolfi, and F. Pederiva, “Hyperon Puzzle: Hints from Quantum Monte Carlo Calculations”, *Phys. Rev. Lett.* **114** (2015) 092301, [arXiv:1407.4448 \[nucl-th\]](#).

- [4] D. Logoteta, I. Vidana, and I. Bombaci, “Impact of chiral hyperonic three-body forces on neutron stars”, *Eur. Phys. J. A* **55** (2019) 207, arXiv:1906.11722 [nucl-th].
- [5] L. Fabbietti, V. Mantovani Sarti, and O. Vazquez Doce, “Study of the Strong Interaction Among Hadrons with Correlations at the LHC”, *Ann. Rev. Nucl. Part. Sci.* **71** (2021) 377–402, arXiv:2012.09806 [nucl-ex].
- [6] ALICE Collaboration, S. Acharya *et al.*, “Unveiling the strong interaction among hadrons at the LHC”, *Nature* **588** (2020) 232–238, arXiv:2005.11495 [nucl-ex]. [Erratum:*Nature* **590** (2021) E13].
- [7] H. Kamada, J. Golak, K. Miyagawa, H. Witala, and W. Gloeckle, “ π -mesonic decay of the hypertriton”, *Phys. Rev. C* **57** (1998) 1595–1603, arXiv:nucl-th/9709035.
- [8] J. Haidenbauer, U. G. Meißner, and A. Nogga, “Hyperon–nucleon interaction within chiral effective field theory revisited”, *Eur. Phys. J. A* **56** (2020) 91, arXiv:1906.11681 [nucl-th].
- [9] D. Lonardonì and F. Pederiva, “Medium-mass hypernuclei and the nucleon-isospin dependence of the three-body hyperon-nucleon-nucleon force”, arXiv:1711.07521 [nucl-th].
- [10] R. J. Prem and P. H. Steinberg, “Lifetimes of hypernuclei, ${}^3_{\Lambda}\text{H}$, ${}^4_{\Lambda}\text{H}$, ${}^5_{\Lambda}\text{H}$ ”, *Physical Review* **136** (1964) B1803–B1806. Publisher: American Physical Society.
- [11] G. Keyes *et al.*, “New Measurement of the ${}^3_{\Lambda}\text{H}$ Lifetime”, *Phys. Rev. Lett.* **20** (1968) 819–821.
- [12] R. E. Phillips and J. Schneps, “Lifetimes of light hyperfragments. II”, *Phys. Rev.* **180** (1969) 1307–1318.
- [13] G. Bohm *et al.*, “On the lifetime of the ${}^3_{\Lambda}\text{H}$ hypernucleus”, *Nucl. Phys. B* **16** (1970) 46–52. [Erratum: *Nucl.Phys.B* 16 (1970) 523–523].
- [14] G. Keyes, J. Sacton, J. H. Wickens, and M. M. Block, “A measurement of the lifetime of the ${}^3_{\Lambda}\text{H}$ hypernucleus”, *Nucl. Phys. B* **67** (1973) 269–283.
- [15] ALICE Collaboration, J. Adam *et al.*, “ ${}^3_{\Lambda}\text{H}$ and ${}^3_{\Lambda}\bar{\text{H}}$ production in Pb–Pb collisions at $\sqrt{s_{\text{NN}}} = 2.76$ TeV”, *Phys. Lett. B* **754** (2016) 360–372, arXiv:1506.08453 [nucl-ex].
- [16] ALICE Collaboration, S. Acharya *et al.*, “ ${}^3_{\Lambda}\text{H}$ and ${}^3_{\Lambda}\bar{\text{H}}$ lifetime measurement in Pb–Pb collisions at $\sqrt{s_{\text{NN}}} = 5.02$ TeV via two-body decay”, *Phys. Lett. B* **797** (2019) 134905, arXiv:1907.06906 [nucl-ex].
- [17] ALICE Collaboration, S. Acharya *et al.*, “Hypertriton Production in p–Pb Collisions at $\sqrt{s_{\text{NN}}}=5.02$ TeV”, *Phys. Rev. Lett.* **128** (2022) 252003, arXiv:2107.10627 [nucl-ex].
- [18] ALICE Collaboration, S. Acharya *et al.*, “Measurement of the Lifetime and Λ Separation Energy of ${}^3_{\Lambda}\text{H}$ ”, *Phys. Rev. Lett.* **131** (2023) 102302, arXiv:2209.07360 [nucl-ex].
- [19] STAR Collaboration, L. Adamczyk *et al.*, “Measurement of the ${}^3_{\Lambda}\text{H}$ lifetime in Au+Au collisions at the BNL Relativistic Heavy Ion Collider”, *Phys. Rev. C* **97** (2018) 054909, arXiv:1710.00436 [nucl-ex].
- [20] STAR Collaboration, M. Abdallah *et al.*, “Measurements of ${}^3_{\Lambda}\text{H}$ and ${}^4_{\Lambda}\text{H}$ Lifetimes and Yields in Au+Au Collisions in the High Baryon Density Region”, *Phys. Rev. Lett.* **128** (2022) 202301, arXiv:2110.09513 [nucl-ex].
- [21] STAR Collaboration, “Observation of the Antimatter Hypernucleus ${}^4_{\Lambda}\bar{\text{H}}$ ”, arXiv:2310.12674 [nucl-ex].

- [22] P. Eckert *et al.*, “Chart of hypernuclides — Hypernuclear structure and decay data”, 2023. <https://hypernuclei.kph.uni-mainz.de>.
- [23] A. Cobis, A. S. Jensen, and D. V. Fedorov, “The simplest strange three-body halo”, *Journal of Physics G: Nuclear and Particle Physics* **23** (1997) 401.
- [24] H. Nemura, Y. Suzuki, Y. Fujiwara, and C. Nakamoto, “Study of light Λ - and $\Lambda\Lambda$ -hypernuclei with the stochastic variational method and effective ΛN potentials”, *Prog. Theor. Phys.* **103** (2000) 929–958, arXiv:nucl-th/9912065 [nucl-th].
- [25] F. Hildenbrand and H. W. Hammer, “Three-Body Hypernuclei in Pionless Effective Field Theory”, *Phys. Rev. C* **100** (2019) 034002, arXiv:1904.05818 [nucl-th]. [Erratum:Phys.Rev.C 102, 039901 (2020)].
- [26] A. Andronic, P. Braun-Munzinger, K. Redlich, and J. Stachel, “Decoding the phase structure of QCD via particle production at high energy”, *Nature* **561** (2018) 321–330, arXiv:1710.09425 [nucl-th].
- [27] V. Vovchenko, B. Dönigus, and H. Stoecker, “Multiplicity dependence of light nuclei production at LHC energies in the canonical statistical model”, *Phys. Lett. B* **785** (2018) 171–174, arXiv:1808.05245 [hep-ph].
- [28] V. Vovchenko, B. Dönigus, and H. Stoecker, “Canonical statistical model analysis of p–p, p–Pb, and Pb–Pb collisions at energies available at the CERN Large Hadron Collider”, *Phys. Rev. C* **100** (2019) 054906, arXiv:1906.03145 [hep-ph].
- [29] V. Vovchenko and V. Koch, “Centrality dependence of proton and light nuclei yields as a consequence of baryon annihilation in the hadronic phase”, *Phys. Lett. B* **835** (2022) 137577, arXiv:2210.15641 [nucl-th].
- [30] L.-W. Chen, C. M. Ko, and B.-A. Li, “Light cluster production in intermediate-energy heavy ion collisions induced by neutron rich nuclei”, *Nucl. Phys. A* **729** (2003) 809–834, arXiv:nucl-th/0306032.
- [31] K. Blum, K. C. Y. Ng, R. Sato, and M. Takimoto, “Cosmic rays, antihelium, and an old navy spotlight”, *Phys. Rev. D* **96** (2017) 103021, arXiv:1704.05431 [astro-ph.HE].
- [32] F. Bellini and A. P. Kalweit, “Testing coalescence and statistical-thermal production scenarios for (anti-)(hyper-)nuclei and exotic QCD objects at LHC energies”, *Phys. Rev.* **C99** (2019) 054905, arXiv:1807.05894 [hep-ph].
- [33] K.-J. Sun, C. M. Ko, and B. Dönigus, “Suppression of light nuclei production in collisions of small systems at the Large Hadron Collider”, *Phys. Lett. B* **792** (2019) 132–137, arXiv:1812.05175 [nucl-th].
- [34] F. Bellini, K. Blum, A. P. Kalweit, and M. Puccio, “Examination of coalescence as the origin of nuclei in hadronic collisions”, *Phys. Rev. C* **103** (2021) 014907, arXiv:2007.01750 [nucl-th].
- [35] M. Kachelriess, S. Ostapchenko, and J. Tjemsland, “On nuclear coalescence in small interacting systems”, *Eur. Phys. J. A* **57** (2021) 167, arXiv:2012.04352 [hep-ph].
- [36] M. Mahlein *et al.*, “A realistic coalescence model for deuteron production”, *Eur. Phys. J. C* **83** (2023) 804, arXiv:2302.12696 [hep-ex].
- [37] R. Scheibl and U. W. Heinz, “Coalescence and flow in ultrarelativistic heavy ion collisions”, *Phys. Rev. C* **59** (1999) 1585–1602, arXiv:nucl-th/9809092.

- [38] ALICE Collaboration, J. Adam *et al.*, “Production of light nuclei and anti-nuclei in pp and Pb–Pb collisions at energies available at the CERN Large Hadron Collider”, *Phys. Rev. C* **93** (2016) 024917, arXiv:1506.08951 [nucl-ex].
- [39] ALICE Collaboration, S. Acharya *et al.*, “Production of deuterons, tritons, ${}^3\text{He}$ nuclei and their antinuclei in pp collisions at $\sqrt{s} = 0.9, 2.76$ and 7 TeV”, *Phys. Rev. C* **97** (2018) 024615, arXiv:1709.08522 [nucl-ex].
- [40] ALICE Collaboration, S. Acharya *et al.*, “Production of ${}^4\text{He}$ and ${}^4\overline{\text{He}}$ in Pb–Pb collisions at $\sqrt{s_{\text{NN}}} = 2.76$ TeV at the LHC”, *Nucl. Phys. A* **971** (2018) 1–20, arXiv:1710.07531 [nucl-ex].
- [41] ALICE Collaboration, S. Acharya *et al.*, “Measurement of deuteron spectra and elliptic flow in Pb–Pb collisions at $\sqrt{s_{\text{NN}}} = 2.76$ TeV at the LHC”, *Eur. Phys. J. C* **77** (2017) 658, arXiv:1707.07304 [nucl-ex].
- [42] ALICE Collaboration, S. Acharya *et al.*, “Multiplicity dependence of (anti-)deuteron production in pp collisions at $\sqrt{s} = 7$ TeV”, *Phys. Lett. B* **794** (2019) 50–63, arXiv:1902.09290 [nucl-ex].
- [43] ALICE Collaboration, S. Acharya *et al.*, “Production of (anti-) ${}^3\text{He}$ and (anti-) ${}^3\text{H}$ in p–Pb collisions at $\sqrt{s_{\text{NN}}} = 5.02$ TeV”, *Phys. Rev. C* **101** (2020) 044906, arXiv:1910.14401 [nucl-ex].
- [44] ALICE Collaboration, S. Acharya *et al.*, “(Anti-)deuteron production in pp collisions at $\sqrt{s} = 13$ TeV”, *Eur. Phys. J. C* **80** (2020) 889, arXiv:2003.03184 [nucl-ex].
- [45] ALICE Collaboration, S. Acharya *et al.*, “Measurement of the production of (anti)nuclei in p–Pb collisions at $\sqrt{s_{\text{NN}}} = 8.16$ TeV”, *Phys. Lett. B* **846** (2023) 137795, arXiv:2212.04777 [nucl-ex].
- [46] ALICE Collaboration, S. Acharya *et al.*, “Production of light (anti)nuclei in pp collisions at $\sqrt{s} = 13$ TeV”, *JHEP* **01** (2022) 106, arXiv:2109.13026 [nucl-ex].
- [47] ALICE Collaboration, S. Acharya *et al.*, “Production of light (anti)nuclei in pp collisions at $\sqrt{s} = 5.02$ TeV”, *Eur. Phys. J. C* **82** (2022) 289, arXiv:2112.00610 [nucl-ex].
- [48] ALICE Collaboration, S. Acharya *et al.*, “Light (anti)nuclei production in Pb–Pb collisions at $\sqrt{s_{\text{NN}}} = 5.02$ TeV”, *Phys. Rev. C* **107** (2023) 064904, arXiv:2211.14015 [nucl-ex].
- [49] ALICE Collaboration, S. Acharya *et al.*, “Measurement of (anti)alpha production in central Pb–Pb collisions at $\sqrt{s_{\text{NN}}} = 5.02$ TeV”, arXiv:2311.11758 [nucl-ex].
- [50] S. Mrowczynski, “Production of light nuclei at colliders – coalescence vs. thermal model”, *Eur. Phys. J. ST* **229** (2020) 3559–3583, arXiv:2004.07029 [nucl-th].
- [51] J. Rais, H. van Hees, and C. Greiner, “Bound-state formation in time-dependent potentials”, *Phys. Rev. C* **106** (2022) 064004, arXiv:2207.04898 [quant-ph].
- [52] ALICE Collaboration, B. B. Abelev *et al.*, “Performance of the ALICE Experiment at the CERN LHC”, *Int. J. Mod. Phys. A* **29** (2014) 1430044, arXiv:1402.4476 [nucl-ex].
- [53] ALICE Collaboration, K. Aamodt *et al.*, “Alignment of the ALICE Inner Tracking System with cosmic-ray tracks”, *JINST* **5** (2010) P03003, arXiv:1001.0502 [physics.ins-det].
- [54] J. Alme *et al.*, “The ALICE TPC, a large 3-dimensional tracking device with fast readout for ultra-high multiplicity events”, *Nucl. Instrum. Meth. A* **622** (2010) 316–367.

- [55] ALICE Collaboration, E. Abbas *et al.*, “Performance of the ALICE VZERO system”, *JINST* **8** (2013) P10016, arXiv:1306.3130 [nucl-ex].
- [56] ALICE Collaboration, “Centrality determination in heavy ion collisions”, *ALICE-PUBLIC-2018-011* (2018). <https://cds.cern.ch/record/2636623>.
- [57] ALICE Collaboration, S. Acharya *et al.*, “Measurements of chemical potentials in Pb–Pb collisions at $\sqrt{s_{\text{NN}}} = 5.02$ TeV”, arXiv:2311.13332 [nucl-ex].
- [58] X.-N. Wang and M. Gyulassy, “HIJING: A Monte Carlo model for multiple jet production in pp, pA and AA collisions”, *Phys. Rev. D* **44** (1991) 3501–3516.
- [59] E. Schnedermann, J. Sollfrank, and U. W. Heinz, “Thermal phenomenology of hadrons from 200 AGeV S+S collisions”, *Phys. Rev. C* **48** (1993) 2462–2475, arXiv:nucl-th/9307020.
- [60] GEANT4 Collaboration, S. Agostinelli *et al.*, “GEANT4—a simulation toolkit”, *Nucl. Instrum. Meth. A* **506** (2003) 250–303.
- [61] T. Chen and C. Guestrin, “Xgboost: A scalable tree boosting system”, in *Proceedings of the 22nd ACM SIGKDD International Conference on Knowledge Discovery and Data Mining*, KDD ’16, p. 785–794. Association for Computing Machinery, New York, NY, USA, 2016. <https://doi.org/10.1145/2939672.2939785>.
- [62] L. Barioglio, F. Catalano, M. Concas, P. Fecchio, F. Grosa, F. Mazzaschi, and M. Puccio, “hipe4ml/hipe4ml”, Nov., 2021. <https://doi.org/10.5281/zenodo.5734093>.
- [63] W. Verkerke and D. P. Kirkby, “The RooFit toolkit for data modeling”, *eConf* **C0303241** (2003) MOLT007, arXiv:physics/0306116. <https://root.cern.ch/doc/master/classRooCrystalBall.html>.
- [64] M. V. Evlanov, A. M. Sokolov, V. K. Tartakovsky, S. A. Khorozov, and Y. Lukstins, “Interaction of hypertritons with nuclei at high-energies”, *Nucl. Phys. A* **632** (1998) 624–632.
- [65] K. Cranmer, “Kernel estimation in high-energy physics”, *Computer Physics Communications* **136** (2001) 198–207.
- [66] V. Vovchenko and H. Stoecker, “Thermal-FIST: A package for heavy-ion collisions and hadronic equation of state”, *Comput. Phys. Commun.* **244** (2019) 295–310, arXiv:1901.05249 [nucl-th].
- [67] D.-N. Liu *et al.*, “Quantum Mechanical Softening of the Hypertriton Transverse Momentum Spectrum in Heavy-Ion Collisions”, arXiv:2404.02701 [nucl-th].
- [68] ALICE Collaboration, J. Adam *et al.*, “Centrality Dependence of the Charged-Particle Multiplicity Density at Midrapidity in Pb–Pb Collisions at $\sqrt{s_{\text{NN}}} = 5.02$ TeV”, *Phys. Rev. Lett.* **116** (2016) 222302, arXiv:1512.06104 [nucl-ex].

A The ALICE Collaboration

S. Acharya ¹²⁷, D. Adamová ⁸⁶, A. Agarwal¹³⁵, G. Aglieri Rinella ³², L. Aglietta²⁴, M. Agnello ²⁹, N. Agrawal ²⁵, Z. Ahammed ¹³⁵, S. Ahmad ¹⁵, S.U. Ahn ⁷¹, I. Ahuja ³⁷, A. Akindinov ¹⁴¹, V. Akishina³⁸, M. Al-Turany ⁹⁷, D. Aleksandrov ¹⁴¹, B. Alessandro ⁵⁶, H.M. Alfanda ⁶, R. Alfaro Molina ⁶⁷, B. Ali ¹⁵, A. Alici ²⁵, N. Alizadehvandchali ¹¹⁶, A. Alkin ¹⁰⁴, J. Alme ²⁰, G. Alocco ⁵², T. Alt ⁶⁴, A.R. Altamura ⁵⁰, I. Altsybeev ⁹⁵, J.R. Alvarado ⁴⁴, M.N. Anaam ⁶, C. Andrei ⁴⁵, N. Andreou ¹¹⁵, A. Andronic ¹²⁶, E. Andronov ¹⁴¹, V. Anguelov ⁹⁴, F. Antinori ⁵⁴, P. Antonioli ⁵¹, N. Apadula ⁷⁴, L. Aphecetche ¹⁰³, H. Appelshäuser ⁶⁴, C. Arata ⁷³, S. Arcelli ²⁵, M. Aresti ²², R. Arnaldi ⁵⁶, J.G.M.C.A. Arneiro ¹¹⁰, I.C. Arsene ¹⁹, M. Arslanok ¹³⁸, A. Augustinus ³², R. Averbeck ⁹⁷, D. Averyanov ¹⁴¹, M.D. Azmi ¹⁵, H. Baba¹²⁴, A. Badalà ⁵³, J. Bae ¹⁰⁴, Y.W. Baek ⁴⁰, X. Bai ¹²⁰, R. Bailhache ⁶⁴, Y. Bailung ⁴⁸, R. Bala ⁹¹, A. Balbino ²⁹, A. Baldisseri ¹³⁰, B. Balis ², D. Banerjee ⁴, Z. Banoo ⁹¹, V. Barbasova³⁷, F. Barile ³¹, L. Barioglio ⁵⁶, M. Barlou⁷⁸, B. Barman⁴¹, G.G. Barnaföldi ⁴⁶, L.S. Barnby ¹¹⁵, E. Barreau ¹⁰³, V. Barret ¹²⁷, L. Barreto ¹¹⁰, C. Bartels ¹¹⁹, K. Barth ³², E. Bartsch ⁶⁴, N. Bastid ¹²⁷, S. Basu ⁷⁵, G. Batigne ¹⁰³, D. Battistini ⁹⁵, B. Batyunya ¹⁴², D. Bauri⁴⁷, J.L. Bazo Alba ¹⁰¹, I.G. Bearden ⁸³, C. Beattie ¹³⁸, P. Becht ⁹⁷, D. Behera ⁴⁸, I. Belikov ¹²⁹, A.D.C. Bell Hechavarria ¹²⁶, F. Bellini ²⁵, R. Bellwied ¹¹⁶, S. Belokurova ¹⁴¹, L.G.E. Beltran ¹⁰⁹, Y.A.V. Beltran ⁴⁴, G. Bencedi ⁴⁶, A. Bensaoula¹¹⁶, S. Beole ²⁴, Y. Berdnikov ¹⁴¹, A. Berdnikova ⁹⁴, L. Bergmann ⁹⁴, M.G. Besoiu ⁶³, L. Betev ³², P.P. Bhaduri ¹³⁵, A. Bhasin ⁹¹, B. Bhattacharjee ⁴¹, L. Bianchi ²⁴, N. Bianchi ⁴⁹, J. Bielčik ³⁵, J. Bielčíková ⁸⁶, A.P. Bigot ¹²⁹, A. Bilandžić ⁹⁵, G. Biro ⁴⁶, S. Biswas ⁴, N. Bize ¹⁰³, J.T. Blair ¹⁰⁸, D. Blau ¹⁴¹, M.B. Blidaru ⁹⁷, N. Bluhme³⁸, C. Blume ⁶⁴, G. Boca ^{21,55}, F. Bock ⁸⁷, T. Bodova ²⁰, J. Bok ¹⁶, L. Boldizsár ⁴⁶, M. Bombara ³⁷, P.M. Bond ³², G. Bonomi ^{134,55}, H. Borel ¹³⁰, A. Borissov ¹⁴¹, A.G. Borquez Carcamo ⁹⁴, H. Bossi ¹³⁸, E. Botta ²⁴, Y.E.M. Bouziani ⁶⁴, L. Bratrud ⁶⁴, P. Braun-Munzinger ⁹⁷, M. Bregant ¹¹⁰, M. Broz ³⁵, G.E. Bruno ^{96,31}, V.D. Buchakchiev ³⁶, M.D. Buckland ²³, D. Budnikov ¹⁴¹, H. Buesching ⁶⁴, S. Bufalino ²⁹, P. Buhler ¹⁰², N. Burmasov ¹⁴¹, Z. Buthelezi ^{68,123}, A. Bylinkin ²⁰, S.A. Bysiak¹⁰⁷, J.C. Cabanillas Noris ¹⁰⁹, M.F.T. Cabrera¹¹⁶, M. Cai ⁶, H. Caines ¹³⁸, A. Caliva ²⁸, E. Calvo Villar ¹⁰¹, J.M.M. Camacho ¹⁰⁹, P. Camerini ²³, F.D.M. Canedo ¹¹⁰, S.L. Cantway ¹³⁸, M. Carabas ¹¹³, A.A. Carballo ³², F. Carnesecchi ³², R. Caron ¹²⁸, L.A.D. Carvalho ¹¹⁰, J. Castillo Castellanos ¹³⁰, M. Castoldi ³², F. Catalano ³², S. Cattaruzzi ²³, C. Ceballos Sanchez ¹⁴², R. Cerri²⁴, I. Chakaberia ⁷⁴, P. Chakraborty ^{136,47}, S. Chandra ¹³⁵, S. Chapeland ³², M. Chartier ¹¹⁹, S. Chattopadhyay¹³⁵, S. Chattopadhyay ¹³⁵, S. Chattopadhyay ⁹⁹, M. Chen³⁹, T. Cheng ^{97,6}, C. Cheshkov ¹²⁸, V. Chibante Barroso ³², D.D. Chinellato ¹¹¹, E.S. Chizzali ^{II,95}, J. Cho ⁵⁸, S. Cho ⁵⁸, P. Chochula ³², Z.A. Chochulska¹³⁶, D. Choudhury⁴¹, P. Christakoglou ⁸⁴, C.H. Christensen ⁸³, P. Christiansen ⁷⁵, T. Chujo ¹²⁵, M. Ciacco ²⁹, C. Cicalo ⁵², M.R. Ciupek⁹⁷, G. Clai^{III,51}, F. Colamaria ⁵⁰, J.S. Colburn¹⁰⁰, D. Colella ³¹, M. Colocci ²⁵, M. Concas ³², G. Conesa Balbastre ⁷³, Z. Conesa del Valle ¹³¹, G. Contin ²³, J.G. Contreras ³⁵, M.L. Coquet ^{103,130}, P. Cortese ^{133,56}, M.R. Cosentino ¹¹², F. Costa ³², S. Costanza ^{21,55}, C. Cot ¹³¹, J. Crkovská ⁹⁴, P. Crochet ¹²⁷, R. Cruz-Torres ⁷⁴, P. Cui ⁶, M.M. Czarnynoga¹³⁶, A. Dainese ⁵⁴, G. Dange³⁸, M.C. Danisch ⁹⁴, A. Danu ⁶³, P. Das ⁸⁰, P. Das ⁴, S. Das ⁴, A.R. Dash ¹²⁶, S. Dash ⁴⁷, A. De Caro ²⁸, G. de Cataldo ⁵⁰, J. de Cuveland³⁸, A. De Falco ²², D. De Gruttola ²⁸, N. De Marco ⁵⁶, C. De Martin ²³, S. De Pasquale ²⁸, R. Deb ¹³⁴, R. Del Grande ⁹⁵, L. Dello Stritto ³², W. Deng ⁶, K.C. Devereaux¹⁸, P. Dhankher ¹⁸, D. Di Bari ³¹, A. Di Mauro ³², B. Diab ¹³⁰, R.A. Diaz ^{142,7}, T. Dietel ¹¹⁴, Y. Ding ⁶, J. Ditzel ⁶⁴, R. Divià ³², Ø. Djuvsland²⁰, U. Dmitrieva ¹⁴¹, A. Dobrin ⁶³, B. Dönigus ⁶⁴, J.M. Dubinski ¹³⁶, A. Dubla ⁹⁷, P. Dupieux ¹²⁷, N. Dzalaiiova¹³, T.M. Eder ¹²⁶, R.J. Ehlers ⁷⁴, F. Eisenhut ⁶⁴, R. Ejima⁹², D. Elia ⁵⁰, B. Erazmus ¹⁰³, F. Ercolessi ²⁵, B. Espagnon ¹³¹, G. Eulisse ³², D. Evans ¹⁰⁰, S. Evdokimov ¹⁴¹, L. Fabbietti ⁹⁵, M. Faggin ²³, J. Favre ⁷³, F. Fan ⁶, W. Fan ⁷⁴, A. Fantoni ⁴⁹, M. Fasel ⁸⁷, A. Feliciello ⁵⁶, G. Feofilov ¹⁴¹, A. Fernández Téllez ⁴⁴, L. Ferrandi ¹¹⁰, M.B. Ferrer ³², A. Ferrero ¹³⁰, C. Ferrero ^{IV,56}, A. Ferretti ²⁴, V.J.G. Feuillard ⁹⁴, V. Filova ³⁵, D. Finogeev ¹⁴¹, F.M. Fionda ⁵², E. Flatland³², F. Flor ^{138,116}, A.N. Flores ¹⁰⁸, S. Foertsch ⁶⁸, I. Fokin ⁹⁴, S. Fokin ¹⁴¹, U. Follo^{IV,56}, E. Fragiaco ⁵⁷, E. Frajna ⁴⁶, U. Fuchs ³², N. Funicello ²⁸, C. Furget ⁷³, A. Furs ¹⁴¹, T. Fusayasu ⁹⁸, J.J. Gaardhøje ⁸³, M. Gagliardi ²⁴, A.M. Gago ¹⁰¹, T. Gahlaut⁴⁷, C.D. Galvan ¹⁰⁹, D.R. Gangadharan ¹¹⁶, P. Ganoti ⁷⁸, C. Garabatos ⁹⁷, J.M. García⁴⁴, T. García Chávez ⁴⁴, E. García-Solis ⁹, C. Gargiulo ³², P. Gasik ⁹⁷, H.M. Gaur³⁸, A. Gautam ¹¹⁸, M.B. Gay Ducati ⁶⁶, M. Germain ¹⁰³, R.A. Gernhaeuser⁹⁵, C. Ghosh¹³⁵, M. Giacalone ⁵¹, G. Gioachin ²⁹, S.K. Giri¹³⁵, P. Giubellino ^{97,56}, P. Giubileo ²⁷, A.M.C. Glaenger ¹³⁰, P. Glässel ⁹⁴, E. Glimos ¹²², D.J.Q. Goh⁷⁶, V. Gonzalez ¹³⁷, P. Gordeev ¹⁴¹, M. Gorgon ², K. Goswami ⁴⁸,

S. Gotovac³³, V. Grabski⁶⁷, L.K. Graczykowski¹³⁶, E. Grecka⁸⁶, A. Grelli⁵⁹, C. Grigoras³², V. Grigoriev¹⁴¹, S. Grigoryan^{142,1}, F. Grosa³², J.F. Grosse-Oetringhaus³², R. Grosso⁹⁷, D. Grund³⁵, N.A. Grunwald⁹⁴, G.G. Guardiano¹¹¹, R. Guernane⁷³, M. Guilbaud¹⁰³, K. Gulbrandsen⁸³, J.J.W.K. Gumprecht¹⁰², T. Gündem⁶⁴, T. Gunji¹²⁴, W. Guo⁶, A. Gupta⁹¹, R. Gupta⁹¹, R. Gupta⁴⁸, K. Gwizdzial¹³⁶, L. Gyulai⁴⁶, C. Hadjidakis¹³¹, F.U. Haider⁹¹, S. Haidlova³⁵, M. Haldar⁴, H. Hamagaki⁷⁶, A. Hamdi⁷⁴, Y. Han¹³⁹, B.G. Hanley¹³⁷, R. Hannigan¹⁰⁸, J. Hansen⁷⁵, M.R. Haque⁹⁷, J.W. Harris¹³⁸, A. Harton⁹, M.V. Hartung⁶⁴, H. Hassan¹¹⁷, D. Hatzifotiadou⁵¹, P. Hauer⁴², L.B. Havener¹³⁸, E. Hellbär⁹⁷, H. Helstrup³⁴, M. Hemmer⁶⁴, T. Herman³⁵, S.G. Hernandez¹¹⁶, G. Herrera Corral⁸, S. Herrmann¹²⁸, K.F. Hetland³⁴, B. Heybeck⁶⁴, H. Hillemanns³², B. Hippolyte¹²⁹, F.W. Hoffmann⁷⁰, B. Hofman⁵⁹, G.H. Hong¹³⁹, M. Horst⁹⁵, A. Horzyk², Y. Hou⁶, P. Hristov³², P. Huhn⁶⁴, L.M. Huhta¹¹⁷, T.J. Humanic⁸⁸, A. Hutson¹¹⁶, D. Hutter³⁸, M.C. Hwang¹⁸, R. Ilkaev¹⁴¹, M. Inaba¹²⁵, G.M. Innocenti³², M. Ippolitov¹⁴¹, A. Isakov⁸⁴, T. Isidori¹¹⁸, M.S. Islam⁹⁹, S. Iurchenko¹⁴¹, M. Ivanov⁹⁷, M. Ivanov¹³, V. Ivanov¹⁴¹, K.E. Iversen⁷⁵, M. Jablonski², B. Jacak^{18,74}, N. Jacazio²⁵, P.M. Jacobs⁷⁴, S. Jadlovská¹⁰⁶, J. Jadlovsky¹⁰⁶, S. Jaelani⁸², C. Jahnke¹¹⁰, M.J. Jakubowska¹³⁶, M.A. Janik¹³⁶, T. Janson⁷⁰, S. Ji¹⁶, S. Jia¹⁰, F. Jonas⁷⁴, D.M. Jones¹¹⁹, J.M. Jowett^{32,97}, J. Jung⁶⁴, M. Jung⁶⁴, A. Junique³², A. Jusko¹⁰⁰, J. Kaewjai¹⁰⁵, P. Kalinak⁶⁰, A. Kalweit³², A. Karasu Uysal^{7,72}, D. Karatovic⁸⁹, N. Karatzenis¹⁰⁰, O. Karavichev¹⁴¹, T. Karavicheva¹⁴¹, E. Karpechev¹⁴¹, M.J. Karwowska^{32,136}, U. Keschull⁷⁰, R. Keidel¹⁴⁰, M. Keil³², B. Ketzer⁴², S.S. Khade⁴⁸, A.M. Khan¹²⁰, S. Khan¹⁵, A. Khanzadeev¹⁴¹, Y. Kharlov¹⁴¹, A. Khatun¹¹⁸, A. Khuntia³⁵, Z. Khuranova⁶⁴, B. Kileng³⁴, B. Kim¹⁰⁴, C. Kim¹⁶, D.J. Kim¹¹⁷, E.J. Kim⁶⁹, J. Kim¹³⁹, J. Kim⁵⁸, J. Kim^{32,69}, M. Kim¹⁸, S. Kim¹⁷, T. Kim¹³⁹, K. Kimura⁹², A. Kirkova³⁶, S. Kirsch⁶⁴, I. Kisel³⁸, S. Kiselev¹⁴¹, A. Kisiel¹³⁶, J.P. Kitowski², J.L. Klay⁵, J. Klein³², S. Klein⁷⁴, C. Klein-Bösing¹²⁶, M. Kleiner⁶⁴, T. Klemenz⁹⁵, A. Kluge³², C. Kobdaj¹⁰⁵, R. Kohara¹²⁴, T. Kollegger⁹⁷, A. Kondratyev¹⁴², N. Kondratyeva¹⁴¹, J. König⁶⁴, S.A. Königstorfer⁹⁵, P.J. Konopka³², G. Kornakov¹³⁶, M. Korwieser⁹⁵, S.D. Koryciak², C. Koster⁸⁴, A. Kotliarov⁸⁶, N. Kovacic⁸⁹, V. Kovalenko¹⁴¹, M. Kowalski¹⁰⁷, V. Kozuharov³⁶, I. Králik⁶⁰, A. Kravčáková³⁷, L. Krcal^{32,38}, M. Krivda^{100,60}, F. Krizek⁸⁶, K. Krizkova Gajdosova³², C. Krug⁶⁶, M. Krüger⁶⁴, D.M. Krupova³⁵, E. Kryshen¹⁴¹, V. Kučera⁵⁸, C. Kuhn¹²⁹, P.G. Kuijper⁸⁴, T. Kumaoka¹²⁵, D. Kumar¹³⁵, L. Kumar⁹⁰, N. Kumar⁹⁰, S. Kumar³¹, S. Kundu³², P. Kurashvili⁷⁹, A. Kurepin¹⁴¹, A.B. Kurepin¹⁴¹, A. Kuryakin¹⁴¹, S. Kuschpil⁸⁶, V. Kuskov¹⁴¹, M. Kutyla¹³⁶, A. Kuznetsov¹⁴², M.J. Kweon⁵⁸, Y. Kwon¹³⁹, S.L. La Pointe³⁸, P. La Rocca²⁶, A. Lakrathok¹⁰⁵, M. Lamanna³², A.R. Landou⁷³, R. Langoy¹²¹, P. Larionov³², E. Laudi³², L. Lautner^{32,95}, R.A.N. Laveaga¹⁰⁹, R. Lavicka¹⁰², R. Lea^{134,55}, H. Lee¹⁰⁴, I. Legrand⁴⁵, G. LeGras¹²⁶, J. Leibrach³⁸, A.M. Lejeune³⁵, T.M. Lelek², R.C. Lemmon⁸⁵, I. León Monzón¹⁰⁹, M.M. Lesch⁹⁵, E.D. Lesser¹⁸, P. Lévai⁴⁶, M. Li⁶, X. Li¹⁰, B.E. Liang-gilman¹⁸, J. Lien¹²¹, R. Lietava¹⁰⁰, I. Likmeta¹¹⁶, B. Lim²⁴, S.H. Lim¹⁶, V. Lindenstruth³⁸, A. Lindner⁴⁵, C. Lippmann⁹⁷, D.H. Liu⁶, J. Liu¹¹⁹, G.S.S. Liveraro¹¹¹, I.M. Lofnes²⁰, C. Loizides⁸⁷, S. Lokos¹⁰⁷, J. Lömker⁵⁹, X. Lopez¹²⁷, E. López Torres⁷, C. Lotteau¹²⁸, P. Lu^{97,120}, F.V. Lugo⁶⁷, J.R. Luhder¹²⁶, M. Lunardon²⁷, G. Luparello⁵⁷, Y.G. Ma³⁹, M. Mager³², A. Maire¹²⁹, E.M. Majerz², M.V. Makariev³⁶, M. Malaev¹⁴¹, G. Malfattore²⁵, N.M. Malik⁹¹, Q.W. Malik¹⁹, S.K. Malik⁹¹, L. Malinina^{1, VIII, 142}, D. Mallick¹³¹, N. Mallick⁴⁸, G. Mandaglio^{30,53}, S.K. Mandal⁷⁹, A. Manea⁶³, V. Manko¹⁴¹, F. Manso¹²⁷, V. Manzari⁵⁰, Y. Mao⁶, R.W. Marcjan², G.V. Margagliotti²³, A. Margotti⁵¹, A. Marín⁹⁷, C. Markert¹⁰⁸, P. Martinengo³², M.I. Martínez⁴⁴, G. Martínez García¹⁰³, M.P.P. Martins¹¹⁰, S. Masciocchi⁹⁷, M. Maserà²⁴, A. Masoni⁵², L. Massacrier¹³¹, O. Massen⁵⁹, A. Mastroserio^{132,50}, O. Matonoha⁷⁵, S. Mattiazzo²⁷, A. Matyja¹⁰⁷, A.L. Mazuecos³², F. Mazzaschi^{32,24}, M. Mazzilli¹¹⁶, J.E. Mdhuli¹²³, Y. Melikyan⁴³, A. Menchaca-Rocha⁶⁷, J.E.M. Mendez⁶⁵, E. Meninno¹⁰², A.S. Menon¹¹⁶, M.W. Menzel^{32,94}, M. Meres¹³, Y. Miake¹²⁵, L. Micheletti³², D.L. Mihaylov⁹⁵, K. Mikhaylov^{142,141}, N. Minafra¹¹⁸, D. Miśkowiec⁹⁷, A. Modak^{134,4}, B. Mohanty⁸⁰, M. Mohisin Khan^{VI,15}, M.A. Molander⁴³, S. Monira¹³⁶, C. Mordasini¹¹⁷, D.A. Moreira De Godoy¹²⁶, I. Morozov¹⁴¹, A. Morsch³², T. Mrnjavac³², V. Muccifora⁴⁹, S. Muhuri¹³⁵, J.D. Mulligan⁷⁴, A. Mulliri²², M.G. Munhoz¹¹⁰, R.H. Munzer⁶⁴, H. Murakami¹²⁴, S. Murray¹¹⁴, L. Musa³², J. Musinsky⁶⁰, J.W. Myrcha¹³⁶, B. Naik¹²³, A.I. Nambrath¹⁸, B.K. Nandi⁴⁷, R. Nania⁵¹, E. Nappi⁵⁰, A.F. Nassirpour¹⁷, A. Nath⁹⁴, S. Nath¹³⁵, C. Nattrass¹²², M.N. Naydenov³⁶, A. Neagu¹⁹, A. Negru¹¹³, E. Nekrasova¹⁴¹, L. Nellen⁶⁵, R. Nepeivoda⁷⁵, S. Nese¹⁹, G. Neskovic³⁸, N. Nicassio⁵⁰, B.S. Nielsen⁸³, E.G. Nielsen⁸³, S. Nikolaev¹⁴¹, S. Nikulin¹⁴¹, V. Nikulin¹⁴¹, F. Noferini⁵¹, S. Noh¹²,

P. Nomokonov ¹⁴², J. Norman ¹¹⁹, N. Novitzky ⁸⁷, P. Nowakowski ¹³⁶, A. Nyanin ¹⁴¹, J. Nystrand ²⁰, S. Oh ¹⁷, A. Ohlson ⁷⁵, V.A. Okorokov ¹⁴¹, J. Oleniacz ¹³⁶, A. Onnerstad ¹¹⁷, C. Oppedisano ⁵⁶, A. Ortiz Velasquez ⁶⁵, J. Otwinowski ¹⁰⁷, M. Oya ⁹², K. Oyama ⁷⁶, Y. Pachmayer ⁹⁴, S. Padhan ⁴⁷, D. Pagano ^{134,55}, G. Paic̃ ⁶⁵, S. Paisano-Guzman ⁴⁴, A. Palasciano ⁵⁰, S. Panebianco ¹³⁰, H. Park ¹²⁵, H. Park ¹⁰⁴, J. Park ¹²⁵, J.E. Parkkila ³², Y. Patley ⁴⁷, R.N. Patra ⁵⁰, B. Paul ¹³⁵, M.M.D.M. Paulino ¹¹⁰, H. Pei ⁶, T. Peitzmann ⁵⁹, X. Peng ¹¹, M. Pennisi ²⁴, S. Perciballi ²⁴, D. Peresunko ¹⁴¹, G.M. Perez ⁷, Y. Pestov ¹⁴¹, M.T. Petersen ⁸³, V. Petrov ¹⁴¹, M. Petrovici ⁴⁵, S. Piano ⁵⁷, M. Pikna ¹³, P. Pillot ¹⁰³, O. Pinazza ^{51,32}, L. Pinsky ¹¹⁶, C. Pinto ⁹⁵, S. Pisano ⁴⁹, M. Płoskoń ⁷⁴, M. Planinic ⁸⁹, F. Pliquett ⁶⁴, D.K. Plociennik ², M.G. Poghosyan ⁸⁷, B. Polichtchouk ¹⁴¹, S. Politano ²⁹, N. Poljak ⁸⁹, A. Pop ⁴⁵, S. Porteboeuf-Houssais ¹²⁷, V. Pozdniakov ^{1,142}, I.Y. Pozos ⁴⁴, K.K. Pradhan ⁴⁸, S.K. Prasad ⁴, S. Prasad ⁴⁸, R. Preghenella ⁵¹, F. Prino ⁵⁶, C.A. Pruneau ¹³⁷, I. Pshenichnov ¹⁴¹, M. Puccio ³², S. Pucillo ²⁴, S. Qiu ⁸⁴, L. Quaglia ²⁴, S. Ragoni ¹⁴, A. Rai ¹³⁸, A. Rakotozafindrabe ¹³⁰, L. Ramello ^{133,56}, F. Rami ¹²⁹, M. Rasa ²⁶, S.S. Rasanen ⁴³, R. Rath ⁵¹, M.P. Rauch ²⁰, I. Ravasenga ³², K.F. Read ^{87,122}, C. Reckziegel ¹¹², A.R. Redelbach ³⁸, K. Redlich ^{VII,79}, C.A. Reetz ⁹⁷, H.D. Regules-Medel ⁴⁴, A. Rehman ²⁰, F. Reidt ³², H.A. Reme-Ness ³⁴, Z. Rescakova ³⁷, K. Reygers ⁹⁴, A. Riabov ¹⁴¹, V. Riabov ¹⁴¹, R. Ricci ²⁸, M. Richter ²⁰, A.A. Riedel ⁹⁵, W. Riegler ³², A.G. Riffero ²⁴, C. Ripoli ²⁸, C. Ristea ⁶³, M.V. Rodriguez ³², M. Rodrıguez Cahuantzi ⁴⁴, S.A. Rodrıguez Ramırez ⁴⁴, K. Roed ¹⁹, R. Rogalev ¹⁴¹, E. Rogochaya ¹⁴², T.S. Rogoschinski ⁶⁴, D. Rohr ³², D. Rohrich ²⁰, S. Rojas Torres ³⁵, P.S. Rokita ¹³⁶, G. Romanenko ²⁵, F. Ronchetti ⁴⁹, E.D. Rosas ⁶⁵, K. Roslon ¹³⁶, A. Rossi ⁵⁴, A. Roy ⁴⁸, S. Roy ⁴⁷, N. Rubini ^{51,25}, J.A. Rudolph ⁸⁴, D. Ruggiano ¹³⁶, R. Rui ²³, P.G. Russek ², R. Russo ⁸⁴, A. Rustamov ⁸¹, E. Ryabinkin ¹⁴¹, Y. Ryabov ¹⁴¹, A. Rybicki ¹⁰⁷, J. Ryu ¹⁶, W. Rzeska ¹³⁶, B. Sabiu ⁵¹, S. Sadovsky ¹⁴¹, J. Saetre ²⁰, K. Safařık ³⁵, S.K. Saha ⁴, S. Saha ⁸⁰, B. Sahoo ⁴⁸, R. Sahoo ⁴⁸, S. Sahoo ⁶¹, D. Sahu ⁴⁸, P.K. Sahu ⁶¹, J. Saini ¹³⁵, K. Sajdakova ³⁷, S. Sakai ¹²⁵, M.P. Salvan ⁹⁷, S. Sambyal ⁹¹, D. Samitz ¹⁰², I. Sanna ^{32,95}, T.B. Saramela ¹¹⁰, D. Sarkar ⁸³, P. Sarma ⁴¹, V. Sarritzu ²², V.M. Sarti ⁹⁵, M.H.P. Sas ³², S. Sawan ⁸⁰, E. Scapparone ⁵¹, J. Schambach ⁸⁷, H.S. Scheid ⁶⁴, C. Schiaua ⁴⁵, R. Schicker ⁹⁴, F. Schlepper ⁹⁴, A. Schmah ⁹⁷, C. Schmidt ⁹⁷, H.R. Schmidt ⁹³, M.O. Schmidt ³², M. Schmidt ⁹³, N.V. Schmidt ⁸⁷, A.R. Schmier ¹²², R. Schotter ¹²⁹, A. Schroter ³⁸, J. Schukraft ³², K. Schweda ⁹⁷, G. Scioli ²⁵, E. Scomparin ⁵⁶, J.E. Seger ¹⁴, Y. Sekiguchi ¹²⁴, D. Sekihata ¹²⁴, M. Selina ⁸⁴, I. Selyuzhenkov ⁹⁷, S. Senyukov ¹²⁹, J.J. Seo ⁹⁴, D. Serebryakov ¹⁴¹, L. Serkin ⁶⁵, L. ˇSerksnyte ⁹⁵, A. Sevcenco ⁶³, T.J. Shaba ⁶⁸, A. Shabetai ¹⁰³, R. Shahoyan ³², A. Shangaraev ¹⁴¹, B. Sharma ⁹¹, D. Sharma ⁴⁷, H. Sharma ⁵⁴, M. Sharma ⁹¹, S. Sharma ⁷⁶, S. Sharma ⁹¹, U. Sharma ⁹¹, A. Shatat ¹³¹, O. Sheibani ¹¹⁶, K. Shigaki ⁹², M. Shimomura ⁷⁷, J. Shin ¹², S. Shirinkin ¹⁴¹, Q. Shou ³⁹, Y. Sibiriak ¹⁴¹, S. Siddhanta ⁵², T. Siemiarzuk ⁷⁹, T.F. Silva ¹¹⁰, D. Silvermyr ⁷⁵, T. Simantathammakul ¹⁰⁵, R. Simeonov ³⁶, B. Singh ⁹¹, B. Singh ⁹⁵, K. Singh ⁴⁸, R. Singh ⁸⁰, R. Singh ⁹¹, R. Singh ⁹⁷, S. Singh ¹⁵, V.K. Singh ¹³⁵, V. Singhal ¹³⁵, T. Sinha ⁹⁹, B. Sitar ¹³, M. Sitta ^{133,56}, T.B. Skaali ¹⁹, G. Skorodumovs ⁹⁴, N. Smirnov ¹³⁸, R.J.M. Snellings ⁵⁹, E.H. Solheim ¹⁹, J. Song ¹⁶, C. Sonnabend ^{32,97}, J.M. Sonneveld ⁸⁴, F. Soramel ²⁷, A.B. Soto-herandez ⁸⁸, R. Spijkers ⁸⁴, I. Sputowska ¹⁰⁷, J. Staa ⁷⁵, J. Stachel ⁹⁴, I. Stan ⁶³, P.J. Steffanic ¹²², S.F. Stiefelmaier ⁹⁴, D. Stocco ¹⁰³, I. Storehaug ¹⁹, N.J. Strangmann ⁶⁴, P. Stratmann ¹²⁶, S. Strazzi ²⁵, A. Sturniolo ^{30,53}, C.P. Stylianidis ⁸⁴, A.A.P. Suaide ¹¹⁰, C. Suire ¹³¹, M. Sukhanov ¹⁴¹, M. Suljic ³², R. Sultanov ¹⁴¹, V. Sumberia ⁹¹, S. Sumowidagdo ⁸², I. Szarka ¹³, M. Szymkowski ¹³⁶, S.F. Taghavi ⁹⁵, G. Taillepiep ⁹⁷, J. Takahashi ¹¹¹, G.J. Tambave ⁸⁰, S. Tang ⁶, Z. Tang ¹²⁰, J.D. Tapia Takaki ¹¹⁸, N. Tapes ¹¹³, L.A. Tarasovicova ¹²⁶, M.G. Tarzila ⁴⁵, G.F. Tassielli ³¹, A. Tauro ³², A. Tavira Garcıa ¹³¹, G. Tejada Munoz ⁴⁴, A. Telesca ³², L. Terlizzi ²⁴, C. Terrevoli ⁵⁰, S. Thakur ⁴, D. Thomas ¹⁰⁸, A. Tikhonov ¹⁴¹, N. Tiltmann ^{32,126}, A.R. Timmins ¹¹⁶, M. Tkacik ¹⁰⁶, T. Tkacik ¹⁰⁶, A. Toia ⁶⁴, R. Tokumoto ⁹², S. Tomassini ²⁵, K. Tomohiro ⁹², N. Topilskaya ¹⁴¹, M. Toppi ⁴⁹, V.V. Torres ¹⁰³, A.G. Torres Ramos ³¹, A. Trifiro ^{30,53}, T. Triloki ⁹⁶, A.S. Triolo ^{32,30,53}, S. Tripathy ³², T. Tripathy ⁴⁷, V. Trubnikov ³, W.H. Trzaska ¹¹⁷, T.P. Trzcinski ¹³⁶, C. Tsolanta ¹⁹, R. Tu ³⁹, A. Tumkin ¹⁴¹, R. Turrisi ⁵⁴, T.S. Tveter ¹⁹, K. Ullaland ²⁰, B. Ulukutlu ⁹⁵, A. Uras ¹²⁸, M. Urioni ¹³⁴, G.L. Usai ²², M. Vala ³⁷, N. Valle ⁵⁵, L.V.R. van Doremalen ⁵⁹, M. van Leeuwen ⁸⁴, C.A. van Veen ⁹⁴, R.J.G. van Weelden ⁸⁴, P. Vande Vyvre ³², D. Varga ⁴⁶, Z. Varga ⁴⁶, P. Vargas Torres ⁶⁵, M. Vasileiou ⁷⁸, A. Vasiliev ¹⁴¹, O. Vazquez Doce ⁴⁹, O. Vazquez Rueda ¹¹⁶, V. Vechernin ¹⁴¹, E. Vercellin ²⁴, S. Vergara Limon ⁴⁴, R. Verma ⁴⁷, L. Vermunt ⁹⁷, R. Vertesi ⁴⁶, M. Verweij ⁵⁹, L. Vickovic ³³, Z. Vilakazi ¹²³, O. Villalobos Baillie ¹⁰⁰, A. Villani ²³, A. Vinogradov ¹⁴¹, T. Virgili ²⁸, M.M.O. Virta ¹¹⁷, A. Vodopyanov ¹⁴², B. Volkel ³², M.A. Volkl ⁹⁴, S.A. Voloshin ¹³⁷, G. Volpe ³¹, B. von Haller ³², I. Vorobyev ³², N. Vozniuk ¹⁴¹,

J. Vrláková³⁷, J. Wan³⁹, C. Wang³⁹, D. Wang³⁹, Y. Wang³⁹, Y. Wang⁶, A. Wegrzynek³², F.T. Weiglhofer³⁸, S.C. Wenzel³², J.P. Wessels¹²⁶, J. Wiechula⁶⁴, J. Wikne¹⁹, G. Wilk⁷⁹, J. Wilkinson⁹⁷, G.A. Willems¹²⁶, B. Windelband⁹⁴, M. Winn¹³⁰, J.R. Wright¹⁰⁸, W. Wu³⁹, Y. Wu¹²⁰, Z. Xiong¹²⁰, R. Xu⁶, A. Yadav⁴², A.K. Yadav¹³⁵, Y. Yamaguchi⁹², S. Yang²⁰, S. Yano⁹², E.R. Yeats¹⁸, Z. Yin⁶, I.-K. Yoo¹⁶, J.H. Yoon⁵⁸, H. Yu¹², S. Yuan²⁰, A. Yuncu⁹⁴, V. Zaccolo²³, C. Zampolli³², M. Zang⁶, F. Zanone⁹⁴, N. Zardoshti³², A. Zarochentsev¹⁴¹, P. Závada⁶², N. Zaviyalov¹⁴¹, M. Zhalov¹⁴¹, B. Zhang⁶, C. Zhang¹³⁰, L. Zhang³⁹, M. Zhang^{127,6}, S. Zhang³⁹, X. Zhang⁶, Y. Zhang¹²⁰, Z. Zhang⁶, M. Zhao¹⁰, V. Zhrebchevskii¹⁴¹, Y. Zhi¹⁰, D. Zhou⁶, Y. Zhou⁸³, J. Zhu^{54,6}, S. Zhu¹²⁰, Y. Zhu⁶, S.C. Zugravel⁵⁶, N. Zurlo^{134,55}

Affiliation Notes

^I Deceased

^{II} Also at: Max-Planck-Institut für Physik, Munich, Germany

^{III} Also at: Italian National Agency for New Technologies, Energy and Sustainable Economic Development (ENEA), Bologna, Italy

^{IV} Also at: Dipartimento DET del Politecnico di Torino, Turin, Italy

^V Also at: Yildiz Technical University, Istanbul, Türkiye

^{VI} Also at: Department of Applied Physics, Aligarh Muslim University, Aligarh, India

^{VII} Also at: Institute of Theoretical Physics, University of Wrocław, Poland

^{VIII} Also at: An institution covered by a cooperation agreement with CERN

Collaboration Institutes

¹ A.I. Alikhanyan National Science Laboratory (Yerevan Physics Institute) Foundation, Yerevan, Armenia

² AGH University of Krakow, Cracow, Poland

³ Bogolyubov Institute for Theoretical Physics, National Academy of Sciences of Ukraine, Kiev, Ukraine

⁴ Bose Institute, Department of Physics and Centre for Astroparticle Physics and Space Science (CAPSS), Kolkata, India

⁵ California Polytechnic State University, San Luis Obispo, California, United States

⁶ Central China Normal University, Wuhan, China

⁷ Centro de Aplicaciones Tecnológicas y Desarrollo Nuclear (CEADEN), Havana, Cuba

⁸ Centro de Investigación y de Estudios Avanzados (CINVESTAV), Mexico City and Mérida, Mexico

⁹ Chicago State University, Chicago, Illinois, United States

¹⁰ China Institute of Atomic Energy, Beijing, China

¹¹ China University of Geosciences, Wuhan, China

¹² Chungbuk National University, Cheongju, Republic of Korea

¹³ Comenius University Bratislava, Faculty of Mathematics, Physics and Informatics, Bratislava, Slovak Republic

¹⁴ Creighton University, Omaha, Nebraska, United States

¹⁵ Department of Physics, Aligarh Muslim University, Aligarh, India

¹⁶ Department of Physics, Pusan National University, Pusan, Republic of Korea

¹⁷ Department of Physics, Sejong University, Seoul, Republic of Korea

¹⁸ Department of Physics, University of California, Berkeley, California, United States

¹⁹ Department of Physics, University of Oslo, Oslo, Norway

²⁰ Department of Physics and Technology, University of Bergen, Bergen, Norway

²¹ Dipartimento di Fisica, Università di Pavia, Pavia, Italy

²² Dipartimento di Fisica dell'Università and Sezione INFN, Cagliari, Italy

²³ Dipartimento di Fisica dell'Università and Sezione INFN, Trieste, Italy

²⁴ Dipartimento di Fisica dell'Università and Sezione INFN, Turin, Italy

²⁵ Dipartimento di Fisica e Astronomia dell'Università and Sezione INFN, Bologna, Italy

²⁶ Dipartimento di Fisica e Astronomia dell'Università and Sezione INFN, Catania, Italy

²⁷ Dipartimento di Fisica e Astronomia dell'Università and Sezione INFN, Padova, Italy

²⁸ Dipartimento di Fisica 'E.R. Caianiello' dell'Università and Gruppo Collegato INFN, Salerno, Italy

²⁹ Dipartimento DISAT del Politecnico and Sezione INFN, Turin, Italy

³⁰ Dipartimento di Scienze MIFT, Università di Messina, Messina, Italy

³¹ Dipartimento Interateneo di Fisica 'M. Merlin' and Sezione INFN, Bari, Italy

- ³² European Organization for Nuclear Research (CERN), Geneva, Switzerland
- ³³ Faculty of Electrical Engineering, Mechanical Engineering and Naval Architecture, University of Split, Split, Croatia
- ³⁴ Faculty of Engineering and Science, Western Norway University of Applied Sciences, Bergen, Norway
- ³⁵ Faculty of Nuclear Sciences and Physical Engineering, Czech Technical University in Prague, Prague, Czech Republic
- ³⁶ Faculty of Physics, Sofia University, Sofia, Bulgaria
- ³⁷ Faculty of Science, P.J. Šafárik University, Košice, Slovak Republic
- ³⁸ Frankfurt Institute for Advanced Studies, Johann Wolfgang Goethe-Universität Frankfurt, Frankfurt, Germany
- ³⁹ Fudan University, Shanghai, China
- ⁴⁰ Gangneung-Wonju National University, Gangneung, Republic of Korea
- ⁴¹ Gauhati University, Department of Physics, Guwahati, India
- ⁴² Helmholtz-Institut für Strahlen- und Kernphysik, Rheinische Friedrich-Wilhelms-Universität Bonn, Bonn, Germany
- ⁴³ Helsinki Institute of Physics (HIP), Helsinki, Finland
- ⁴⁴ High Energy Physics Group, Universidad Autónoma de Puebla, Puebla, Mexico
- ⁴⁵ Horia Hulubei National Institute of Physics and Nuclear Engineering, Bucharest, Romania
- ⁴⁶ HUN-REN Wigner Research Centre for Physics, Budapest, Hungary
- ⁴⁷ Indian Institute of Technology Bombay (IIT), Mumbai, India
- ⁴⁸ Indian Institute of Technology Indore, Indore, India
- ⁴⁹ INFN, Laboratori Nazionali di Frascati, Frascati, Italy
- ⁵⁰ INFN, Sezione di Bari, Bari, Italy
- ⁵¹ INFN, Sezione di Bologna, Bologna, Italy
- ⁵² INFN, Sezione di Cagliari, Cagliari, Italy
- ⁵³ INFN, Sezione di Catania, Catania, Italy
- ⁵⁴ INFN, Sezione di Padova, Padova, Italy
- ⁵⁵ INFN, Sezione di Pavia, Pavia, Italy
- ⁵⁶ INFN, Sezione di Torino, Turin, Italy
- ⁵⁷ INFN, Sezione di Trieste, Trieste, Italy
- ⁵⁸ Inha University, Incheon, Republic of Korea
- ⁵⁹ Institute for Gravitational and Subatomic Physics (GRASP), Utrecht University/Nikhef, Utrecht, Netherlands
- ⁶⁰ Institute of Experimental Physics, Slovak Academy of Sciences, Košice, Slovak Republic
- ⁶¹ Institute of Physics, Homi Bhabha National Institute, Bhubaneswar, India
- ⁶² Institute of Physics of the Czech Academy of Sciences, Prague, Czech Republic
- ⁶³ Institute of Space Science (ISS), Bucharest, Romania
- ⁶⁴ Institut für Kernphysik, Johann Wolfgang Goethe-Universität Frankfurt, Frankfurt, Germany
- ⁶⁵ Instituto de Ciencias Nucleares, Universidad Nacional Autónoma de México, Mexico City, Mexico
- ⁶⁶ Instituto de Física, Universidade Federal do Rio Grande do Sul (UFRGS), Porto Alegre, Brazil
- ⁶⁷ Instituto de Física, Universidad Nacional Autónoma de México, Mexico City, Mexico
- ⁶⁸ iThemba LABS, National Research Foundation, Somerset West, South Africa
- ⁶⁹ Jeonbuk National University, Jeonju, Republic of Korea
- ⁷⁰ Johann-Wolfgang-Goethe Universität Frankfurt Institut für Informatik, Fachbereich Informatik und Mathematik, Frankfurt, Germany
- ⁷¹ Korea Institute of Science and Technology Information, Daejeon, Republic of Korea
- ⁷² KTO Karatay University, Konya, Turkey
- ⁷³ Laboratoire de Physique Subatomique et de Cosmologie, Université Grenoble-Alpes, CNRS-IN2P3, Grenoble, France
- ⁷⁴ Lawrence Berkeley National Laboratory, Berkeley, California, United States
- ⁷⁵ Lund University Department of Physics, Division of Particle Physics, Lund, Sweden
- ⁷⁶ Nagasaki Institute of Applied Science, Nagasaki, Japan
- ⁷⁷ Nara Women's University (NWU), Nara, Japan
- ⁷⁸ National and Kapodistrian University of Athens, School of Science, Department of Physics, Athens, Greece
- ⁷⁹ National Centre for Nuclear Research, Warsaw, Poland
- ⁸⁰ National Institute of Science Education and Research, Homi Bhabha National Institute, Jatni, India
- ⁸¹ National Nuclear Research Center, Baku, Azerbaijan
- ⁸² National Research and Innovation Agency - BRIN, Jakarta, Indonesia

- ⁸³ Niels Bohr Institute, University of Copenhagen, Copenhagen, Denmark
⁸⁴ Nikhef, National institute for subatomic physics, Amsterdam, Netherlands
⁸⁵ Nuclear Physics Group, STFC Daresbury Laboratory, Daresbury, United Kingdom
⁸⁶ Nuclear Physics Institute of the Czech Academy of Sciences, Husinec-Řež, Czech Republic
⁸⁷ Oak Ridge National Laboratory, Oak Ridge, Tennessee, United States
⁸⁸ Ohio State University, Columbus, Ohio, United States
⁸⁹ Physics department, Faculty of science, University of Zagreb, Zagreb, Croatia
⁹⁰ Physics Department, Panjab University, Chandigarh, India
⁹¹ Physics Department, University of Jammu, Jammu, India
⁹² Physics Program and International Institute for Sustainability with Knotted Chiral Meta Matter (SKCM2), Hiroshima University, Hiroshima, Japan
⁹³ Physikalisches Institut, Eberhard-Karls-Universität Tübingen, Tübingen, Germany
⁹⁴ Physikalisches Institut, Ruprecht-Karls-Universität Heidelberg, Heidelberg, Germany
⁹⁵ Physik Department, Technische Universität München, Munich, Germany
⁹⁶ Politecnico di Bari and Sezione INFN, Bari, Italy
⁹⁷ Research Division and ExtreMe Matter Institute EMMI, GSI Helmholtzzentrum für Schwerionenforschung GmbH, Darmstadt, Germany
⁹⁸ Saga University, Saga, Japan
⁹⁹ Saha Institute of Nuclear Physics, Homi Bhabha National Institute, Kolkata, India
¹⁰⁰ School of Physics and Astronomy, University of Birmingham, Birmingham, United Kingdom
¹⁰¹ Sección Física, Departamento de Ciencias, Pontificia Universidad Católica del Perú, Lima, Peru
¹⁰² Stefan Meyer Institut für Subatomare Physik (SMI), Vienna, Austria
¹⁰³ SUBATECH, IMT Atlantique, Nantes Université, CNRS-IN2P3, Nantes, France
¹⁰⁴ Sungkyunkwan University, Suwon City, Republic of Korea
¹⁰⁵ Suranaree University of Technology, Nakhon Ratchasima, Thailand
¹⁰⁶ Technical University of Košice, Košice, Slovak Republic
¹⁰⁷ The Henryk Niewodniczanski Institute of Nuclear Physics, Polish Academy of Sciences, Cracow, Poland
¹⁰⁸ The University of Texas at Austin, Austin, Texas, United States
¹⁰⁹ Universidad Autónoma de Sinaloa, Culiacán, Mexico
¹¹⁰ Universidade de São Paulo (USP), São Paulo, Brazil
¹¹¹ Universidade Estadual de Campinas (UNICAMP), Campinas, Brazil
¹¹² Universidade Federal do ABC, Santo Andre, Brazil
¹¹³ Universitatea Nationala de Stiinta si Tehnologie Politehnica Bucuresti, Bucharest, Romania
¹¹⁴ University of Cape Town, Cape Town, South Africa
¹¹⁵ University of Derby, Derby, United Kingdom
¹¹⁶ University of Houston, Houston, Texas, United States
¹¹⁷ University of Jyväskylä, Jyväskylä, Finland
¹¹⁸ University of Kansas, Lawrence, Kansas, United States
¹¹⁹ University of Liverpool, Liverpool, United Kingdom
¹²⁰ University of Science and Technology of China, Hefei, China
¹²¹ University of South-Eastern Norway, Kongsberg, Norway
¹²² University of Tennessee, Knoxville, Tennessee, United States
¹²³ University of the Witwatersrand, Johannesburg, South Africa
¹²⁴ University of Tokyo, Tokyo, Japan
¹²⁵ University of Tsukuba, Tsukuba, Japan
¹²⁶ Universität Münster, Institut für Kernphysik, Münster, Germany
¹²⁷ Université Clermont Auvergne, CNRS/IN2P3, LPC, Clermont-Ferrand, France
¹²⁸ Université de Lyon, CNRS/IN2P3, Institut de Physique des 2 Infinis de Lyon, Lyon, France
¹²⁹ Université de Strasbourg, CNRS, IPHC UMR 7178, F-67000 Strasbourg, France, Strasbourg, France
¹³⁰ Université Paris-Saclay, Centre d'Etudes de Saclay (CEA), IRFU, Département de Physique Nucléaire (DPhN), Saclay, France
¹³¹ Université Paris-Saclay, CNRS/IN2P3, IJCLab, Orsay, France
¹³² Università degli Studi di Foggia, Foggia, Italy
¹³³ Università del Piemonte Orientale, Vercelli, Italy
¹³⁴ Università di Brescia, Brescia, Italy
¹³⁵ Variable Energy Cyclotron Centre, Homi Bhabha National Institute, Kolkata, India

¹³⁶ Warsaw University of Technology, Warsaw, Poland

¹³⁷ Wayne State University, Detroit, Michigan, United States

¹³⁸ Yale University, New Haven, Connecticut, United States

¹³⁹ Yonsei University, Seoul, Republic of Korea

¹⁴⁰ Zentrum für Technologie und Transfer (ZTT), Worms, Germany

¹⁴¹ Affiliated with an institute covered by a cooperation agreement with CERN

¹⁴² Affiliated with an international laboratory covered by a cooperation agreement with CERN.